



# Identification of differential anti-neoplastic activity of copper bis(thiosemicarbazones) that is mediated by intracellular reactive oxygen species generation and lysosomal membrane permeabilization



Christian Stefani, Zaynab Al-Eisawi, Patric J. Jansson, Danuta S. Kalinowski\*, Des R. Richardson\*

Molecular Pharmacology and Pathology Program, Department of Pathology and Bosch Institute, The University of Sydney, Sydney, NSW 2006, Australia

## ARTICLE INFO

### Article history:

Received 29 June 2015

Accepted 5 August 2015

Available online 17 August 2015

### Keywords:

Copper

Bis(thiosemicarbazone)

Reactive oxygen species

Lysosome

Lysosomal membrane permeabilization

## ABSTRACT

Bis(thiosemicarbazones) and their copper (Cu) complexes possess unique anti-neoplastic properties. However, their mechanism of action remains unclear. We examined the structure–activity relationships of twelve bis(thiosemicarbazones) to elucidate factors regarding their anti-cancer efficacy. Importantly, the alkyl substitutions at the diimine position of the ligand backbone resulted in two distinct groups, namely, unsubstituted/monosubstituted and disubstituted bis(thiosemicarbazones). This alkyl substitution pattern governed their: (1) Cu<sup>II/I</sup> redox potentials; (2) ability to induce cellular <sup>64</sup>Cu release; (3) lipophilicity; and (4) anti-proliferative activity. The potent anti-cancer Cu complex of the unsubstituted bis(thiosemicarbazone) analog, glyoxal bis(4-methyl-3-thiosemicarbazone) (GTSM), generated intracellular reactive oxygen species (ROS), which was attenuated by Cu sequestration by a non-toxic Cu chelator, tetrathiomolybdate, and the anti-oxidant, *N*-acetyl-L-cysteine. Fluorescence microscopy suggested that the anti-cancer activity of Cu(GTSM) was due, in part, to lysosomal membrane permeabilization (LMP). For the first time, this investigation highlights the role of ROS and LMP in the anti-cancer activity of bis(thiosemicarbazones).

© 2015 Elsevier Inc. All rights reserved.

## 1. Introduction

Copper (Cu) is an essential trace element that plays a key role in the biochemistry of all living organisms [1]. Its unique electronic structure, existing in both an oxidized (Cu<sup>II</sup>) and reduced state (Cu<sup>I</sup>), allows it to serve as a co-factor for enzymes that are fundamental for cellular growth and development [1]. Neoplastic cells have a higher requirement for Cu, as it plays an important role in promoting physiological and malignant angiogenesis [2]. Thus, Cu is essential in the *de novo* formation of blood vessels that enable tumor growth, invasion and metastasis [2]. Further underscoring the importance of Cu in tumor growth is the presence of elevated Cu levels in the serum and tumors of rats and humans [3–5]. Elevated Cu levels in cancer patients have been observed in a wide spectrum of tumors, including: breast [3], cervical [6], ovarian [6], lung [7], prostate [8], colorectal cancer [9] and leukemia [10]. Most strikingly, Cu levels were found to correlate with cancer stage and/or progression [3,9].

Neoplastic cells also differ from their normal counterparts in terms of their redox metabolism [11]. The environment of the tumor is often characterized by increased metabolic activity [12], hypoxia [13] and enhanced intracellular reactive oxygen species (ROS) generation [14].

Importantly, excess Cu is a potent oxidant and results in the generation of cytotoxic ROS in cells [15]. Considering the key role of Cu in both promoting angiogenesis and the generation of ROS, the development of Cu targeting agents has become a promising anti-cancer strategy [15].

Thiosemicarbazones are one such class of promising anti-cancer agents that have attracted extensive interest [16–21]. In particular, the di-2-pyridylketone thiosemicarbazone (DpT) series (e.g., di-2-pyridylketone 4,4-dimethyl-3-thiosemicarbazone; Dp44mT; Fig. 1A) has demonstrated marked and selective anti-tumor activity *in vitro* and *in vivo* against a variety of human tumor xenografts in mice [19, 22]. The mechanism of action of Dp44mT is partly dependent on the formation of a redox active iron complex that generates cytotoxic ROS, leading to damage of essential biomolecules [22–24]. More recently, the Cu(Dp44mT) complex was identified to exhibit superior intracellular oxidative properties and anti-cancer efficacy relative to both the ligand alone and its Fe<sup>III</sup> complex [25]. Additionally, the Cu(Dp44mT) complex was shown to target lysosomal integrity, leading to lysosomal membrane permeabilization (LMP), the redistribution of the lysosomal protease, cathepsin D, to the cytosol and ultimately results in apoptosis [26]. Tumor cell invasion and metastasis involves changes in lysosomal trafficking and increased expression of cathepsins, and it has been suggested that this may sensitize tumor cells to LMP and lysosomal-targeting anti-cancer agents [27,28].

Bis(thiosemicarbazones) are another family of ligands that have also attracted considerable interest due to their broad pharmacological

\* Corresponding authors.

E-mail addresses: [danutak@med.usyd.edu.au](mailto:danutak@med.usyd.edu.au) (D.S. Kalinowski), [d.richardson@med.usyd.edu.au](mailto:d.richardson@med.usyd.edu.au) (D.R. Richardson).

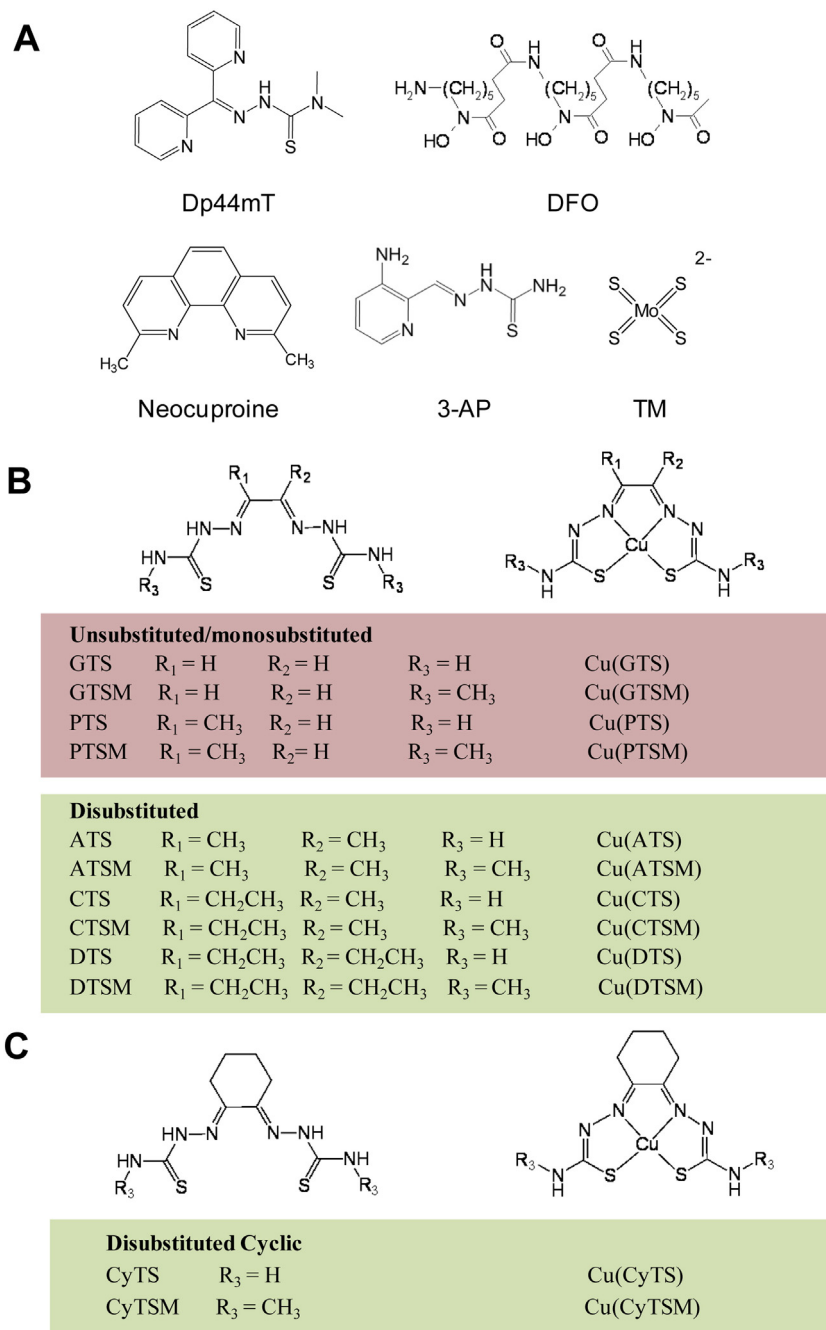


**Fig. 1.** (A) Line drawings of the chemical structures of: di-2-pyridylketone 4,4-dimethyl-3-thiosemicarbazone (Dp44mT), desferrioxamine (DFO), neocuproine (Neo), Triapine (3-AP), and tetrathiomolybdate (TM). (B, C) Line drawings of the chemical structures of members of the bis(thiosemicarbazone) series of ligands and their copper complexes. Throughout the article the unsubstituted/monosubstituted ligands/complexes are indicated in red, while the disubstituted and disubstituted cyclic ligands are denoted in green. (For interpretation of the references to color in this figure legend, the reader is referred to the web version of this article.)

efficacy [29–32]. Their anti-tumor activity was first demonstrated in 1958, after oral administration of glyoxal bis(thiosemicarbazone) (GTS; Fig. 1B) was found to significantly reduce Sarcoma 180 tumor burden in Swiss brown mice [30]. Following the synthesis and evaluation of numerous analogs, kethoxal bis(thiosemicarbazone) emerged as a promising candidate that consistently increased the lifespan of Swiss brown mice with L1210 leukemia [29]. The anti-cancer activity of these ligands was later confirmed in numerous *in vitro* and *in vivo* studies [31–33].

Although not fully elucidated, the mechanism of action of these bis(thiosemicarbazones) is believed to be dependent on Cu coordination, particularly Cu<sup>II</sup> [32,34]. Co-treatment of bis(thiosemicarbazones)

with Cu has been shown to enhance their ability to inhibit DNA synthesis in sarcoma 180 ascites cells [32], as well as their anti-tumor activity against Walker 256 carcinoma in rats [35]. Coordination of Cu by bis(thiosemicarbazones) leads to the formation of a neutral Cu<sup>II</sup>[bis(thiosemicarbazone)] complex, which is capable of rapidly entering cells [36,37]. Once inside the cell, it is proposed that intracellular reduction of the neutral Cu<sup>II</sup>[bis(thiosemicarbazone)] complex to a charged Cu<sup>I</sup> complex occurs, resulting in intracellular trapping [20]. The reduced Cu<sup>I</sup> complex is then believed to either dissociate, or be re-oxidized via a redox-dependent process to the neutral Cu<sup>II</sup> complex, which can be released from the cell [38]. This model is supported by density functional theory [39] and X-ray crystallographic [40] studies

of the ligands and their Cu<sup>II</sup> complexes in cell-free investigations. However, to our knowledge, this reduction and dissociation, leading to intracellular trapping, has not been demonstrated in cells.

Recent interest in bis(thiosemicarbazones) has centered around the hypoxia selectivity of Cu<sup>II</sup> diacetylbis(thiosemicarbazone) (Cu[ATSM]; Fig. 1B) and its potential as a radiopharmaceutical for imaging hypoxic tissues [37,41]. In fact, Cu[ATSM] has demonstrated potential in assessing tumor hypoxia, and thus, prognosis in cervical cancer [42] and rectal carcinoma [43] by positron emission tomography. In fact, the low oxygen tension of hypoxic cells is proposed to stabilize the charged Cu<sup>I</sup> complex, resulting in intracellular accumulation and hypoxia selectivity [20]. However, despite this new medical application, their precise intracellular mechanism of action remains elusive.

Imaging of fluorescent analogs of bis(thiosemicarbazones) has proved an attractive strategy for the study of their *in vitro* subcellular localization [44–47]. A fluorescent pyrene conjugated derivative of Cu(ATSM) has revealed localization into distinct punctuate structures that partially co-localized with lysosome/autophagic structures in HeLa and M17 neuroblastoma cells [48]. In contrast, Cu(ATSM) analogs with a fluorescent naphthoquinone backbone were dispersed evenly in the cytoplasm of HeLa cells [46]. However, the significance of these localization studies on the mechanism of action of the unconjugated complexes is unclear and requires further investigation.

In the present study, we examined a series of bis(thiosemicarbazones) and their Cu<sup>II</sup> complexes (Fig. 1B, C) for their anti-proliferative activity in SK-N-MC neuroepithelioma and mortal MRC-5 fibroblast cells. This series of bis(thiosemicarbazone) ligands and complexes were synthesized to investigate the effect of different structural features on electrochemical and intracellular behavior, including their ability to affect the cellular retention of <sup>64</sup>Cu. The bis(thiosemicarbazone) ligands vary in their alkyl substitution pattern at their diimine backbone (R<sub>1</sub> and R<sub>2</sub>) and their terminal amines (R<sub>3</sub>; Fig. 1B, C). This substitution pattern at R<sub>1</sub> and R<sub>2</sub>, resulted in two major groups of ligands, namely: the unsubstituted/monosubstituted group and the disubstituted group (denoted in red and green, respectively, throughout the study; Fig. 1B, C).

These two groups of ligands had distinct chemical and biological activity that was linked to their Cu<sup>II/I</sup> redox potentials, Cu mobilization activity and lipophilicity. The unsubstituted/monosubstituted bis(thiosemicarbazones) that were less lipophilic and had less negative Cu<sup>II/I</sup> redox potentials resulted in cellular <sup>64</sup>Cu accumulation and greater anti-proliferative efficacy relative to the disubstituted group, that were more lipophilic and had more negative redox potentials. Furthermore, the Cu complex of the unsubstituted bis(thiosemicarbazone) analog, glyoxal bis(4-methyl-3-thiosemicarbazone) (GTSM), that exhibited potent anti-cancer activity, demonstrated the ability to mediate intracellular ROS generation and LMP. For the first time, we demonstrate the anti-proliferative activity of the unsubstituted bis(thiosemicarbazone) ligand, GTSM, is linked with the ability of the resultant Cu complex to redox cycle and mediate LMP.

## 2. Materials and methods

All reagents were obtained commercially and used without further purification. The chelators, Dp44mT and 3-aminopyridine-2-carboxaldehyde thiosemicarbazone (3-AP; Fig. 1A), were prepared and characterized according to previously described methods [23,49,50]. All synthesized compounds were ≥95% purity.

### 2.1. Physical methods

<sup>1</sup>H NMR (400 MHz) spectra were acquired using a Bruker Advance 400 NMR spectrometer with DMSO-*d*<sub>6</sub> as the solvent and internal reference (Me<sub>2</sub>SO: <sup>1</sup>H NMR δ 2.50 ppm and <sup>13</sup>C NMR δ 39.5 ppm vs. TMS). Cyclic voltammetry was performed using a BAS100B/W potentiostat. A glassy carbon working electrode, an aqueous Ag/AgCl reference and Pt wire auxiliary electrode were used. All complexes were at ca. 2 mM

concentration in DMSO. The supporting electrolyte was Et<sub>4</sub>NClO<sub>4</sub> (0.1 M) and the solutions were purged with nitrogen prior to measurement. Partition coefficients of the free ligands were determined by ChemBioDraw v.11.0.1. (PerkinElmer, Waltham, MA, USA) using Crippen's fragmentation procedure [51].

### 2.2. General synthesis of ligands

The ligands were synthesized by the following common procedure, exemplified by the synthetic route used for glyoxalbis(thiosemicarbazone) (GTS). Thiosemicarbazide (10 mmol) was dissolved in ethanol (10 mL) and the appropriate diketone (5 mmol) was dissolved in ethanol (5 mL) and the two solutions then mixed. Glacial acetic acid (5–6 drops) was added and the mixture gently refluxed for 2 to 5 h. The mixture was cooled to room temperature and allowed to stand at 4 °C overnight to ensure complete precipitation. The product was filtered off and washed with distilled water (2 × 10 mL) and ethanol (10 mL) and dried *in vacuo*.

#### 2.2.1. Glyoxalbis(thiosemicarbazone) (GTS)

Pale yellow powder (yield: 82.1%). Anal. Calc. for C<sub>4</sub>H<sub>8</sub>N<sub>6</sub>S<sub>2</sub>: C, 23.5; H, 4.0; N, 41.1; S, 31.4%. Found: C, 23.6; H, 4.1; N, 41.2; S, 31.2%. <sup>1</sup>H NMR (DMSO-*d*<sub>6</sub>): 11.68 (s, 2H), 8.30 (s, 2H), 7.88 (s, 2H), 7.70 (s, 2H). MS (ESI<sup>+</sup>) *m/z* 205.3 [M + H]<sup>+</sup>, 227.3 [M + Na]<sup>+</sup>, 243.4 [M + K]<sup>+</sup>.

#### 2.2.2. Glyoxalbis(4-methyl-3-thiosemicarbazone) (GTSM)

Yellow powder (yield: 85%). Anal. Calc. for C<sub>6</sub>H<sub>12</sub>N<sub>6</sub>S<sub>2</sub>: C, 31.0; H, 5.2; N, 36.2; S, 27.6%. Found: C, 31.0; H, 5.4; N, 36.4; S, 27.9%. <sup>1</sup>H NMR (DMSO-*d*<sub>6</sub>): 11.74 (s, 2H), 8.49 (q, 2H), 7.71 (s, 2H), 2.95 (d, 6H). MS (ESI<sup>+</sup>) *m/z* 233.4 [M + H]<sup>+</sup>, 255.4 [M + Na]<sup>+</sup>, 271.4 [M + K]<sup>+</sup>.

#### 2.2.3. Pyruvaldehydebis(thiosemicarbazone) (PTS)

Pale yellow powder (yield: 74.3%). Anal. Calc. for C<sub>5</sub>H<sub>10</sub>N<sub>6</sub>S<sub>2</sub>: C, 27.5; H, 4.6; N, 38.5; S, 29.4%. Found: C, 27.2; H, 4.8; N, 38.2; S, 29.6%. <sup>1</sup>H NMR (DMSO-*d*<sub>6</sub>): 11.66 (s, 1H), 10.38 (s, 1H), 8.35 (d, 2H), 7.91 (s, 2H), 7.65 (s, 1H), 2.13 (s, 3H). MS (ESI<sup>+</sup>) *m/z* 241.3 [M + Na]<sup>+</sup>, 257.4 [M + K]<sup>+</sup>.

#### 2.2.4. Pyruvaldehydebis(4-methyl-3-thiosemicarbazone) (PTSM)

Pale yellow powder (yield: 78.5%). Anal. Calc. for C<sub>7</sub>H<sub>14</sub>N<sub>6</sub>S<sub>2</sub>: C, 34.1; H, 5.7; N, 34.1; S, 26.0%. Found: C, 34.0; H, 5.9; N, 34.0; S, 26.3%. <sup>1</sup>H NMR (DMSO-*d*<sub>6</sub>): 11.72 (s, 1H), 10.36 (s, 1H), 8.48 (q, 2H), 7.65 (s, 1H), 2.99 (d, 6H), 2.15 (s, 3H). MS (ESI<sup>+</sup>) *m/z* 247.4 [M + H]<sup>+</sup>, 269.4 [M + Na]<sup>+</sup>, 285.4 [M + K]<sup>+</sup>.

#### 2.2.5. Diacetylbis(thiosemicarbazone) (ATS)

Pale yellow powder (yield: 80.5%). Anal. Calc. for C<sub>6</sub>H<sub>12</sub>N<sub>6</sub>S<sub>2</sub>: C, 31.0; H, 5.2; N, 36.2; S, 27.6%. Found: C, 31.0; H, 5.4; N, 36.2; S, 27.4%. <sup>1</sup>H NMR (DMSO-*d*<sub>6</sub>): 10.21 (s, 2H), 8.41 (s, 2H), 7.85 (s, 2H), 2.16 (s, 6H). MS (ESI<sup>+</sup>) *m/z* 233.4 [M + H]<sup>+</sup>, 255.4 [M + Na]<sup>+</sup>, 271.4 [M + K]<sup>+</sup>.

#### 2.2.6. Diacetylbis(4-methyl-3-thiosemicarbazone) (ATSM)

Pale yellow powder (yield: 82.2%). Anal. Calc. for C<sub>8</sub>H<sub>16</sub>N<sub>6</sub>S<sub>2</sub>: C, 36.9; H, 6.2; N, 32.3; S, 24.6%. Found: C, 36.7; H, 6.3; N, 32.1; S, 24.5%. <sup>1</sup>H NMR (DMSO-*d*<sub>6</sub>): 10.22 (s, 2H), 8.37 (q, 2H), 3.01 (d, 6H), 2.20 (s, 6H). MS (ESI<sup>+</sup>) *m/z* 283.4 [M + Na]<sup>+</sup>, 299.4 [M + K]<sup>+</sup>.

#### 2.2.7. 2,3-Pentanedionebis(thiosemicarbazone) (CTS)

Pale yellow powder (yield: 82.8%). Anal. Calc. for C<sub>7</sub>H<sub>14</sub>N<sub>6</sub>S<sub>2</sub>: C, 34.1; H, 5.7; N, 34.1; S, 26.0%. Found: C, 34.3; H, 5.9; N, 34.0; S, 25.9%. <sup>1</sup>H NMR (DMSO-*d*<sub>6</sub>): 10.35 (s, 1H), 10.22 (s, 1H), 8.42 (s, 2H), 7.80 (d, 2H), 2.84 (q, 2H), 2.14 (s, 3H), 0.89 (t, 3H). MS (ESI<sup>+</sup>) *m/z* 269.4 [M + Na]<sup>+</sup>, 285.4 [M + K]<sup>+</sup>.

#### 2.2.8. 2,3-Pentanedionebis(4-methyl-3-thiosemicarbazone) (CTSM)

Yellow powder (yield: 91%). Anal. Calculated for C<sub>9</sub>H<sub>18</sub>N<sub>6</sub>S<sub>2</sub>: C, 39.4; H, 6.6; N, 30.6; S, 23.4%. Found: C, 39.1; H, 6.9; N, 30.7; S, 23.2%. (DMSO-

$d_6$ ): 10.35 (s, 1H), 10.22 (s, 1H), 8.33 (q, 2H), 3.02 (d, 6H), 2.91 (q, 2H), 2.19 (s, 3H), 0.89 (t, 3H). MS (ESI<sup>+</sup>)  $m/z$  297.4 [M + Na]<sup>+</sup>, 313.4 [M + K]<sup>+</sup>.

### 2.2.9. 3,4-Hexanedionebis(thiosemicarbazone) (DTS)

Pale yellow powder (yield: 84.3%). Anal. Calc. for C<sub>8</sub>H<sub>16</sub>N<sub>6</sub>S<sub>2</sub>: C, 36.9; H, 6.2; N, 32.3; S, 24.6%. Found: C, 37.1; H, 6.5; N, 32.0; S, 24.4%. <sup>1</sup>H NMR (DMSO- $d_6$ ): 10.37 (s, 2H), 8.42 (s, 2H), 7.75 (s, 2H), 2.82 (q, 4H), 0.87 (t, 6H). MS (ESI<sup>+</sup>)  $m/z$  261.4 [M + H]<sup>+</sup>, 283.4 [M + Na]<sup>+</sup>, 299.4 [M + K]<sup>+</sup>.

### 2.2.10. 3,4-Hexanedionebis(4-methyl-3-thiosemicarbazone) (DTSM)

Yellow powder (yield: 91.6%). Anal. Calc. for C<sub>10</sub>H<sub>20</sub>N<sub>6</sub>S<sub>2</sub>: C, 41.6; H, 7.0; N, 29.1; S, 22.2%. Found: C, 41.4; H, 7.2; N, 29.0; S, 22.4%. <sup>1</sup>H NMR (DMSO- $d_6$ ): 10.35 (s, 2H), 8.29 (q, 2H), 3.02 (d, 6H), 2.89 (q, 4H), 0.88 (t, 6H). MS (ESI<sup>+</sup>)  $m/z$  289.5 [M + H]<sup>+</sup>, 311.4 [M + Na]<sup>+</sup>, 327.4 [M + K]<sup>+</sup>.

### 2.2.11. 1,2-Cyclohexanedionebis(thiosemicarbazone) (CyTS)

Dark yellow powder (yield: 80.5%). Anal. Calc. for C<sub>8</sub>H<sub>14</sub>N<sub>6</sub>S<sub>2</sub>: C, 37.2; H, 5.5; N, 32.5; S, 24.8%. Found: C, 37.0; H, 5.7; N, 32.3; S, 25.0%. <sup>1</sup>H NMR (DMSO- $d_6$ ): 10.60 (s, 1H), 9.99 (s, 1H), 8.39 (d, 2H), 8.01 (s, 2H), 2.52 (td, 4H), 1.66 (t, 4H). MS (ESI<sup>+</sup>)  $m/z$  259.4 [M + H]<sup>+</sup>, 281.4 [M + Na]<sup>+</sup>, 297.4 [M + K]<sup>+</sup>.

### 2.2.12. 1,2-Cyclohexanedionebis(4-methyl-3-thiosemicarbazone) (CyTSM)

Dark yellow/orange powder (yield: 87.2%). Anal. Calc. for C<sub>10</sub>H<sub>18</sub>N<sub>6</sub>S<sub>2</sub>: C, 41.9; H, 6.3; N, 29.3; S, 22.4%. Found: C, 41.9; H, 6.4; N, 29.2; S, 22.1%. <sup>1</sup>H NMR (DMSO- $d_6$ ): 10.57 (s, 1H), 10.01 (s, 1H), 8.48 (q, 6H), 2.95 (d, 2H), 2.54 (td, 4H), 1.65 (t, 4H). MS (ESI<sup>+</sup>)  $m/z$  287.4 [M + H]<sup>+</sup>, 309.4 [M + Na]<sup>+</sup>, 325.3 [M + K]<sup>+</sup>.

## 2.3. General synthesis of [Cu<sup>II</sup>(L)] complexes

The Cu complexes were prepared by the following general method [14,20,36], exemplified by the preparation of Cu(GTS): GTS (1 mmol) was dissolved in EtOH (10 mL). Copper chloride (1 mmol), dissolved in EtOH (5 mL), was added and the reaction mixture gently refluxed for 3 h. The mixture was cooled to room temperature and left to stir overnight. The dark red/brown powder was collected by filtration, washed with EtOH (2 × 10 mL) and diethyl ether (10 mL) and dried *in vacuo*. The product was then recrystallized from EtOH/H<sub>2</sub>O or AcCN/H<sub>2</sub>O.

### 2.3.1. Cu(GTS)

Yield: 72%. Anal. Calc. for CuC<sub>4</sub>H<sub>7</sub>N<sub>6</sub>S<sub>2</sub>Cl: C, 15.9%; H, 2.2%; N, 27.8%; Found: C, 16.3%; H, 2.0%; N, 27.5%. MS (EI)  $m/z$  266 [M]<sup>+</sup>.

### 2.3.2. Cu(GTSM)

Yield: 67%. Anal. Calc. for CuC<sub>6</sub>H<sub>10</sub>N<sub>6</sub>S<sub>2</sub>·0.25H<sub>2</sub>O: C, 24.2%; H, 3.6%; N, 28.2%; Found: C, 24.6%; H, 3.5%; N, 28.1%. MS (ESI<sup>+</sup>)  $m/z$  295 [M + H]<sup>+</sup>.

### 2.3.3. Cu(PTS)

Yield: 63%. Anal. Calc. for CuC<sub>5</sub>H<sub>8</sub>N<sub>6</sub>S<sub>2</sub>·0.25CH<sub>3</sub>CN·H<sub>2</sub>O: C, 21.4%; H, 3.5%; N, 28.4%; Found: C, 21.6%; H, 2.9%; N, 28.6%. MS (EI)  $m/z$  280 [M]<sup>+</sup>.

### 2.3.4. Cu(PTSM)

Yield: 71%. Anal. Calc. for CuC<sub>7</sub>H<sub>12</sub>N<sub>6</sub>S<sub>2</sub>·0.25H<sub>2</sub>O: C, 26.9%; H, 4.0%; N, 26.9%; Found: C, 27.3%; H, 3.9%; N, 26.7%. MS (ESI<sup>+</sup>)  $m/z$  309 [M + H]<sup>+</sup>, 330 [M + Na]<sup>+</sup>.

### 2.3.5. Cu(ATS)

Yield: 59%. Anal. Calc. for CuC<sub>6</sub>H<sub>10</sub>N<sub>6</sub>S<sub>2</sub>·0.5H<sub>2</sub>O: C, 23.8%; H, 3.7%; N, 27.7%; Found: C, 24.2%; H, 3.3%; N, 27.4%. MS (ESI<sup>-</sup>)  $m/z$  294 [M]<sup>-</sup>.

### 2.3.6. Cu(ATSM)

Yield: 67%. Anal. Calc. for CuC<sub>8</sub>H<sub>14</sub>N<sub>6</sub>S<sub>2</sub>·0.25H<sub>2</sub>O: C, 29.5%; H, 4.5%; N, 25.8%; Found: C, 29.9%; H, 4.3%; N, 25.6%. MS (ESI<sup>+</sup>)  $m/z$  322 [M + H]<sup>+</sup>.

### 2.3.7. Cu(CTS)

Yield: 70%. Anal. Calc. for CuC<sub>7</sub>H<sub>13</sub>N<sub>6</sub>S<sub>2</sub>Cl·0.25MeCN: C, 25.4%; H, 3.9%; N, 24.7%; Found: C, 25.5%; H, 3.6%; N, 24.8%. MS (EI)  $m/z$  308 [M]<sup>+</sup>.

### 2.3.8. Cu(CTSM)

Yield: 78%. Anal. Calc. for CuC<sub>9</sub>H<sub>17</sub>N<sub>6</sub>S<sub>2</sub>Cl·0.75MeCN: C, 31.3%; H, 4.8%; N, 23.5%; Found: C, 31.1%; H, 4.6%; N, 23.6%. MS (ESI<sup>+</sup>)  $m/z$  336 [M + H]<sup>+</sup>.

### 2.3.9. Cu(DTS)

Yield: 64%. Anal. Calc. for CuC<sub>8</sub>H<sub>14</sub>N<sub>6</sub>S<sub>2</sub>Cl·0.25MeCN: C, 27.7%; H, 4.3%; N, 23.8%; Found: C, 27.4%; H, 4.0%; N, 23.4%. MS (ESI<sup>+</sup>)  $m/z$  322 [M + H]<sup>+</sup>.

### 2.3.10. Cu(DTSM)

Yield: 59%. Anal. Calc. for CuC<sub>10</sub>H<sub>18</sub>N<sub>6</sub>S<sub>2</sub>: C, 34.3%; H, 5.2%; N, 24.0%; Found: C, 34.4%; H, 5.1%; N, 23.9%. MS (ESI<sup>+</sup>)  $m/z$  350 [M + H]<sup>+</sup>.

### 2.3.11. Cu(CyTS)

Yield: 73%. Anal. Calc. for CuC<sub>8</sub>H<sub>12</sub>N<sub>6</sub>S<sub>2</sub>Cl·0.66MeCN: C, 29.2%; H, 3.9%; N, 24.3%; Found: C, 29.1%; H, 3.9%; N, 24.4%. MS (ESI<sup>+</sup>)  $m/z$  320 [M + H]<sup>+</sup>.

### 2.3.12. Cu(CyTSM)

Yield: 79%. Anal. Calc. for CuC<sub>10</sub>H<sub>16</sub>N<sub>6</sub>S<sub>2</sub>·0.25EtOH: C, 35.1%; H, 4.9%; N, 23.4%; Found: C, 34.7%; H, 4.6%; N, 23.5%. MS (ESI<sup>+</sup>)  $m/z$  348 [M + H]<sup>+</sup>.

## 2.4. Biological studies

### 2.4.1. Cell culture

Chelators were dissolved in DMSO as 10 mM stock solutions and diluted in medium containing 10% fetal calf serum (Commonwealth Serum Laboratories, Melbourne, Australia) so that the final [DMSO] < 0.5% (v/v). At this final concentration, DMSO had no effect on proliferation, as shown previously [52]. Human SK-N-MC neuroepithelioma cells and mortal human MRC5 fibroblasts (American Type Culture Collection, Manassas, VA) were grown by standard procedures [22,52] at 37 °C in a humidified atmosphere of 5% CO<sub>2</sub>/95% air in an incubator (Forma Scientific, Marietta, OH).

### 2.4.2. Effect of the chelators on cellular proliferation

The effect of the chelators and complexes on cellular proliferation was determined by the [1-(4,5-dimethylthiazol-2-yl)-2,5-diphenyl tetrazolium] (MTT) assay using standard techniques [52,53]. The SK-N-MC neuroepithelioma and MRC-5 fibroblast cell lines were seeded in 96-well microtiter plates at 1.5 × 10<sup>4</sup> and 1.0 × 10<sup>4</sup> cells/well, respectively, in medium containing chelators or complexes at a range of concentrations (0.0015–25 μM). The cells were incubated at 37 °C in a humidified atmosphere containing 5% CO<sub>2</sub> and 95% air for 72 h. After this incubation, 10 μL of MTT (5 mg/mL) was added to each well and further incubated for 2 h/37 °C. After solubilization of the cells with 100 μL of 10% SDS-50% isobutanol in 10 mM HCl, the plates were read at 570 nm using a scanning multi-well spectrophotometer. The inhibitory concentration (IC<sub>50</sub>) was defined as the chelator concentration necessary to reduce the absorbance to 50% of the untreated control. Using this method, absorbance was shown to be directly proportional to cell counts, as shown previously [52]. To examine the role of Cu chelation and redox stress on anti-proliferative activity, SK-N-MC cells were incubated for 72 h/37 °C with chelators or complexes at a range of concentrations (0–6.25 μM) in the presence of tetrathiomolybdate (TM; 5 μM), *N*-acetyl-L-cysteine (NAC; 5 mM) or buthionine sulfoximine (BSO;

100  $\mu\text{M}$ ) [54,55]. Cells were incubated with control medium, NAC, or TM for 10 min/37 °C prior to incubation with chelators or their respective copper complexes, while BSO was incubated for 16 h/37 °C prior to the addition of ligands or their copper complexes.

#### 2.4.3. Bis(thiosemicarbazone)-mediated $^{64}\text{Cu}$ efflux from cells pre-labeled with $^{64}\text{Cu}$

The ability of chelators to mobilize  $^{64}\text{Cu}$  (ANSTO, Sydney, Australia) from pre-labeled cells were performed by standard methods [26,56]. Briefly, cells were pre-labeled for 1 h/37 °C with  $^{64}\text{Cu}$  (10  $\mu\text{Ci}/\text{mL}$ ;  $^{64}\text{CuCl}_2$ ), washed 4 times on ice and reincubated with medium (control) or medium containing chelators (25  $\mu\text{M}$ ) for 1 h/37 °C. Radioactivity was measured in the cells and supernatant using a  $\gamma$ -scintillation counter (Wallac Wizard 3; Perkin Elmer).

#### 2.4.4. Release of $^{64}\text{Cu}$ from cells pre-labeled with the $^{64}\text{Cu}$ [bis(thiosemicarbazone)] complexes

Complexes were prepared by adding equimolar equivalents of  $^{64}\text{Cu}$  (10  $\mu\text{Ci}/\text{mL}$ ;  $^{64}\text{CuCl}_2$ ; ANSTO) and bis(thiosemicarbazone) chelator. SK-N-MC cells were incubated with the complexes (25  $\mu\text{M}$ ) for 1 h/37 °C, washed 4 times on ice, reincubated for 1 h/37 °C in control media, and the percentage of  $^{64}\text{Cu}$  remaining cell associated assessed [26]. Radioactivity was measured in the cells and supernatant using a  $\gamma$ -scintillation counter (Wallac Wizard 3; PerkinElmer).

#### 2.4.5. Intracellular ROS measurements

Intracellular ROS generation was measured using 2',7'-dichlorodihydrofluorescein diacetate ( $\text{H}_2\text{DCF-DA}$ ) [22,57].  $\text{H}_2\text{DCF-DA}$  is hydrolyzed by intracellular esterases to the membrane impermeable analog, 2',7'-dichlorodihydrofluorescein ( $\text{H}_2\text{DCF}$ ), which leads to its accumulation within the cytosol. Cellular oxidants localized to the cytosol oxidize non-fluorescent  $\text{H}_2\text{DCF}$  to the fluorescent product, dichlorofluorescein (DCF) [22,57]. SK-N-MC cells were incubated with 30 nM  $\text{H}_2\text{DCF-DA}$  for 30 min/37 °C and then washed twice with ice-cold PBS. The cells were then treated with either the positive control,  $\text{H}_2\text{O}_2$  (50  $\mu\text{M}$ ) for 30 min/37 °C, GTSM (2 or 25  $\mu\text{M}$ ), or Cu(GTSM) (5  $\mu\text{M}$ ) for 1 h/37 °C. To examine the effect of Cu and Cu chelation, a 10 min/37 °C pre-incubation of cells with  $\text{CuCl}_2$  (5  $\mu\text{M}$ ) or TM (5  $\mu\text{M}$ ) was used, respectively, prior to further chelator or complex incubation. Cells were collected for flow cytometric assessment and intracellular ROS was detected as an increase in green cytosolic DCF fluorescence with a FACS Canto flow cytometer (Becton Dickinson, Lincoln Park, NJ, USA). In these studies, 10,000 events were acquired for every sample. Data analysis was performed using FlowJo software v7.5.5 (Tree Star Inc., Ashland, OR).

#### 2.4.6. Assessment of lysosomal membrane permeability

Distribution of acridine orange (AO; Sigma-Aldrich) was used to determine LMP as previously described and was quantified with ImageJ v1.48 (Wayne Rasband NIH, USA) [26,58]. Briefly, cells were incubated for 15 min/37 °C with AO (20 mM) then washed 3 times with PBS. The cells were then incubated for 1 h/37 °C with chelators (2 to 25  $\mu\text{M}$ ) with or without a 10 min/37 °C pre-incubation with  $\text{CuCl}_2$  (5  $\mu\text{M}$ ) prior to chelator addition. To examine the role of redox stress in LMP, cells were pre-incubated with NAC (5 mM) or TM (5  $\mu\text{M}$ ) for 10 min/37 °C prior to treatment, while BSO (100  $\mu\text{M}$ ) was pre-incubated for 16 h/37 °C [54,55]. Samples were examined with a Zeiss Axio Observer.Z1 fluorescence microscope (Zeiss, Oberkochen, Germany) equipped with FITC and Texas Red filters. Images were captured with an AxioCam camera and AxioVision Rel. 4.7 Software (Zeiss).

#### 2.4.7. Immunofluorescence studies of lysosomal membrane permeabilization

Lysosomal permeability was examined using immunofluorescence by following lysosomal cathepsin D release as previously reported [58,59]. Lysosome-associated membrane protein 2 (Lamp2) was used

to examine co-localization with lysosomes as previously reported [59–61]. Cells were plated on cover slips ( $1 \times 10^5$  cells/mL) and allowed to grow overnight. To examine the role of redox stress in LMP, cells were pre-treated with TM (5  $\mu\text{M}$ ), NAC (5 mM) and/or BSO (100  $\mu\text{M}$ ) [54,55, 62]. Cells were pre-incubated with NAC or TM for 10 min/37 °C, or with BSO for 16 h/37 °C, prior to chelator incubation. Following washing, the cells were pre-incubated with  $\text{CuCl}_2$  (5  $\mu\text{M}$ ) for 10 min/37 °C followed by incubation with GTSM (2  $\mu\text{M}$ ) and incubated for 1 h/37 °C followed by paraformaldehyde fixation (4%/15 min) and digitonin permeabilization (100  $\mu\text{M}/10$  min). After blocking with 5% bovine serum albumin, immunocytochemistry was performed with anti-cathepsin D (Abcam, USA) and anti-Lamp2 (Abcam, USA) antibodies. The cells were examined with a Zeiss Axio Observer Z1 fluorescence microscope (Zeiss, Germany) equipped with FITC, Texas Red and DAPI filters. Images were captured with an AxioCam camera and AxioVision Rel. 4.7 Software (Zeiss, Germany). Quantification of fluorescence was performed with the image processing and analysis software, ImageJ v1.48.

#### 2.5. Statistical analysis

Experimental data were compared using Student's *t*-test. Results were expressed as mean  $\pm$  SD (number of experiments) and considered to be statistically significant when  $p < 0.05$ .

### 3. Results and discussion

#### 3.1. Preparation and characterization

All ligands were prepared by high yielding Schiff base condensation reactions following a previous synthetic procedure for related bis(thiosemicarbazones) [20]. These compounds were synthesized by refluxing the appropriate thiosemicarbazide with the 1,2-diketone in a 2:1 molar ratio in an acidic EtOH solution. The resulting bis(thiosemicarbazones) were found to be only sparingly soluble in water. However, they exhibited greater solubility in polar aprotic solvents such as DMF, MeCN and DMSO. The  $^1\text{H}$  NMR, mass spectrometry and combustion analyses were consistent with their proposed structures (Fig. 1B). The  $\text{Cu}^{\text{II}}$  complexes were prepared by refluxing  $\text{CuCl}_2$  with the appropriate ligand in a 1:1 molar ratio in ethanol [20]. The complexes showed greater water solubility than the ligand, and were very soluble in polar organic solvents, such as DMF and DMSO.

#### 3.2. Electrochemistry

The electrochemical properties of the Cu complexes of bis(thiosemicarbazones) have important ramifications on their anti-proliferative effects [14,20,36]. Previous structure–activity studies [20,36,39,40] examining the cellular uptake of Cu(ATSM) and related complexes have demonstrated that changes in backbone alkylation can dramatically alter the biological properties of the resultant Cu complex. This effect is believed to be largely due to changes to the redox potential of the Cu complex [14,20,36]. Previous studies have noted a redox potential-dependent rate of reduction, with more negative potentials favoring slower reduction rates, while more positive redox potentials resulted in faster reduction rates [20,36,37]. In addition, computer modeling studies examining the competition between dissociation and re-oxidation of the Cu complexes demonstrated that Cu complexes with more negative redox potentials favored re-oxidation, whereas those with more positive potentials favored dissociation [20]. Thus, we investigated the electrochemical properties of the Cu complexes of all synthesized ligands by cyclic voltammetry and the results are summarized in Table 1 and presented in Fig. 2A. In these studies, 0.1 M  $\text{Et}_4\text{NClO}_4$  in DMSO was chosen as the solvent of choice because of the low aqueous solubility of some of the compounds.

All synthesized Cu complexes exhibited reversible, one electron  $\text{Cu}^{\text{II/I}}$  couples (Fig. 2A). Ligands with no or one alkyl group at  $\text{R}_1$  and  $\text{R}_2$  (*i.e.*,

**Table 1**

Partition coefficients ( $\text{Log } P_{\text{calc}}$ ) and  $\text{Cu}^{\text{II/I}}$  redox potentials of the ligands and Cu complexes, respectively.  $\text{Log } P_{\text{calc}}$  values were calculated using the program ChemBioDrawUltra v11.0.1 using Crippen's fragmentation procedure [51].

Ligand	Partition coefficient ( $\text{Log } P_{\text{calc}}$ )	$\text{Cu}^{\text{II/I}}$ redox potential (V vs. NHE)
<i>Unsubstituted/monosubstituted</i>		
GTS	0.45	−0.43
GTSM	0.84	−0.43
PTS	0.53	−0.50
PTSM	1.45	−0.51
<i>Disubstituted</i>		
ATS	0.65	−0.59
ATSM	1.48	−0.59
CTS	1.34	−0.59
CTSM	2.69	−0.58
DTS	1.69	−0.59
DTSM	2.34	−0.60
CyTS	2.15	−0.62
CyTSM	2.78	−0.62

unsubstituted and monosubstituted ligands, respectively; Fig. 1B; denoted in red) include Cu(GTS), Cu(GTSM), Cu(PTS) and Cu(PTSM). These complexes exhibited more positive  $\text{Cu}^{\text{II/I}}$  redox potentials between −0.43 and −0.51 V (Table 1; Fig. 2A). Of these Cu complexes, Cu(GTS) and Cu(GTSM) possessed the most positive  $\text{Cu}^{\text{II/I}}$  redox potential of −0.43 V (Table 1). The addition of a methyl group at  $R_1$  (*i.e.*, Cu(PTS) and Cu(PTSM)) resulted in more negative  $\text{Cu}^{\text{II/I}}$  redox potentials (−0.50 to −0.51 V; Table 1). Interestingly, previous studies examining the redox active DpT series of thiosemicarbazones have observed  $\text{Cu}^{\text{II/I}}$  redox couples in a similar range as these Cu[bis(thiosemicarbazones)] derived from unsubstituted or monosubstituted ligands [24].

All complexes with alkyl groups at the  $R_1$  and  $R_2$  sites (*i.e.*, disubstituted ligands; Fig. 1B, C; denoted in green), including Cu(ATS), Cu(ATSM), Cu(CTS), Cu(CTSM), Cu(DTS), Cu(DTSM), Cu(CyTS) and Cu(CyTSM), demonstrated completely reversible one electron reductions ( $\text{Cu}^{\text{II/I}}$ ) between −0.58 and −0.62 V (Table 1). Alteration of the length of the substituents on the diimine backbone, from methyl to ethyl, did not appreciably affect  $\text{Cu}^{\text{II/I}}$  redox potentials (Table 1). The incorporation of a six-membered ring into the diimine backbone in CyTS

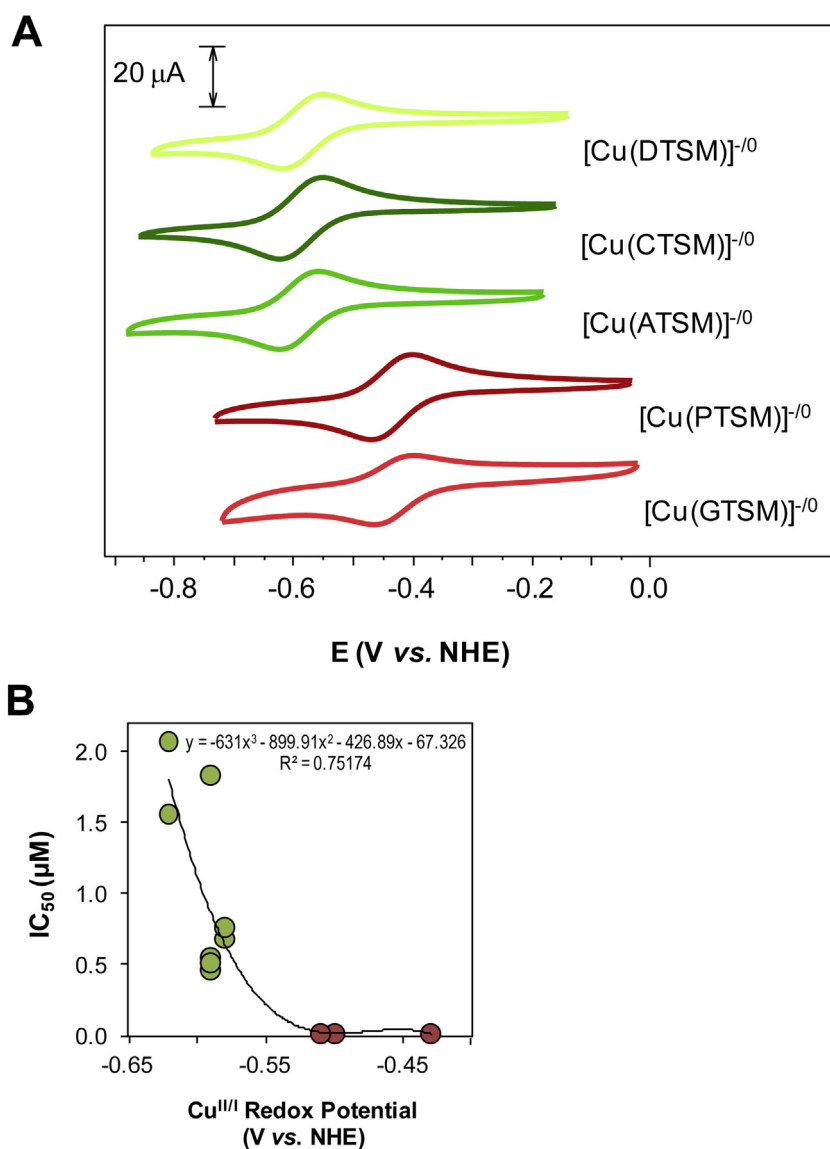


**Fig. 2.** (A) Cyclic voltammograms of 2 mM solutions of: [Cu(DTSM)], [Cu(CTSM)], [Cu(ATSM)], [Cu(PTSM)], and [Cu(GTSM)] (from top to bottom), showing the impact of the diimine backbone alkyl substituents on the  $\text{Cu}^{\text{II/I}}$  redox potential. Sweep rate  $10 \text{ mVs}^{-1}$ , solvent  $0.1 \text{ M Et}_4\text{NClO}_4$  in DMSO. (B) The relationship between the  $\text{Cu}^{\text{II/I}}$  redox potential and the anti-proliferative activity ( $\text{IC}_{50}$ ) of Cu[bis(thiosemicarbazones)].

and CyTSM (Fig. 1C) resulted in the lowest (most negative)  $\text{Cu}^{\text{II}}$  redox potential obtained ( $-0.62$  V; Table 1).

In summary, the  $\text{Cu}[\text{bis}(\text{thiosemicarbazones})]$  complexes can be divided into two groups: (1) those derived from unsubstituted or monosubstituted ligands with more positive  $\text{Cu}^{\text{II}}$  redox couples ( $-0.43$  to  $-0.51$  V; Table 1); and (2) those derived from disubstituted ligands with more negative  $\text{Cu}^{\text{II}}$  redox couples ( $-0.58$  to  $-0.62$  V; Table 1). These results suggest that the  $\text{Cu}$  complexes derived from unsubstituted or monosubstituted ligands, with more positive  $\text{Cu}^{\text{II}}$  redox couples, may be more easily and rapidly reduced to form the charged  $\text{Cu}^{\text{I}}(\text{L})^-$  complex relative to  $\text{Cu}$  complexes of the disubstituted ligands. The differences in the electrochemical behavior of the  $\text{Cu}[\text{bis}(\text{thiosemicarbazone})]$  complexes from unsubstituted and monosubstituted versus disubstituted ligands will probably result in important differences in their ability to mediate ROS formation and induce anti-proliferative activity (examined below).

### 3.3. Biological studies

#### 3.3.1. Anti-proliferative activity of the bis(thiosemicarbazone) ligands against cancer cells

The ability of the bis(thiosemicarbazone) series to inhibit cellular proliferation was assessed using SK-N-MC neuroepithelioma cells, as the effect of other thiosemicarbazones and related aroylhydrazones on these cells has been extensively examined [23,52,63]. Hence, they are a well established model that enables comparisons to our previous studies. These ligands were compared to a number of relevant positive controls, including: (1) Dp44mT (Fig. 1A), a thiosemicarbazone with potent anti-proliferative activity and chelation efficacy that has been extensively studied as an anti-cancer agent [22,64]; (2) desferrioxamine (DFO; Fig. 1A), used for the treatment of Fe overload [64]; and (3) 3-AP (Fig. 1A) that has been investigated as an anti-cancer agent in clinical trials [65–67]. In these studies, SK-N-MC cells were treated with various concentrations (0.0015–25  $\mu\text{M}$ ) of the ligands and incubated for 72 h/37 °C. The concentration of the ligands that reduced cellular proliferation to 50% of the untreated control ( $\text{IC}_{50}$  value) was determined and the results are presented in Table 2.

All bis(thiosemicarbazone) ligands derived from glyoxal and pyruvaldehyde (*i.e.*, the unsubstituted or monosubstituted ligands), namely: GTS, GTSM, PTS and PTSM (Fig. 1B) demonstrated potent anti-proliferative activity against SK-N-MC cells ( $\text{IC}_{50}$ : 0.017–0.021  $\mu\text{M}$ ; Table 2). The anti-proliferative activity of this subset of

ligands was significantly ( $p < 0.001$ ) greater than DFO ( $\text{IC}_{50}$ : 22.7  $\pm$  1.6  $\mu\text{M}$ ), but was significantly ( $p < 0.01$ ) less than that of Dp44mT ( $\text{IC}_{50}$ : 0.004  $\pm$  0.001  $\mu\text{M}$ ; Table 2). Importantly, these unsubstituted or monosubstituted ligands demonstrated significantly ( $p < 0.01$ ) greater anti-proliferative activity than 3-AP ( $\text{IC}_{50}$ : 0.36  $\pm$  0.03  $\mu\text{M}$ ; Table 2). In contrast, the analogs with alkyl substituents at both the  $\text{R}_1$  and  $\text{R}_2$  sites on the diimine backbone (*i.e.*, ATS, ATSM, CTS, CTSM, DTS, DTSM, CyTS and CyTSM), demonstrated very poor anti-proliferative effects against SK-N-MC cells ( $\text{IC}_{50}$ :  $\geq 11.15$   $\mu\text{M}$ ; Table 2).

#### 3.3.2. Anti-proliferative activity of the copper complexes $[\text{Cu}^{\text{II}}(\text{L})]$ against cancer cells

Previous studies have shown that complexation of bis(thiosemicarbazone) ligands with metals results in marked changes in biological activity [32,68,69]. To assess the importance of  $\text{Cu}$  chelation on the anti-proliferative activity of the synthesized ligands, their  $\text{Cu}^{\text{II}}$  complexes were prepared and their anti-proliferative activity was assessed against SK-N-MC neuroepithelioma cells (Table 2). The  $\text{Cu}$  complex of Dp44mT,  $[\text{Cu}(\text{Dp44mT})]\text{Cl}$ , was also included as a control, as its potent anti-proliferative activity has previously been characterized [24–26].

Similarly to their respective ligands, the  $\text{Cu}^{\text{II}}$  complexes derived from unsubstituted or monosubstituted ligands (*i.e.*,  $\text{Cu}(\text{GTS})$ ,  $\text{Cu}(\text{GTSM})$ ,  $\text{Cu}(\text{PTS})$  and  $\text{Cu}(\text{PTSM})$ ), possessed potent anti-proliferative activity against SK-N-MC cells ( $\text{IC}_{50}$ : 0.009–0.016  $\mu\text{M}$ ; Table 2). However, the anti-proliferative activity of these complexes was significantly ( $p < 0.01$ ) less than that of  $\text{Cu}(\text{Dp44mT})$ , which resulted in an  $\text{IC}_{50}$  of 0.004  $\pm$  0.001  $\mu\text{M}$  (Table 2). Although  $\text{Cu}(\text{GTSM})$  ( $\text{IC}_{50}$ : 0.009  $\pm$  0.001  $\mu\text{M}$ ; Table 2) showed significantly ( $p < 0.05$ ) increased anti-proliferative activity relative to the ligand alone (GTSM; 0.020  $\pm$  0.004  $\mu\text{M}$ ; Table 2), the other  $\text{Cu}^{\text{II}}$  complexes derived from unsubstituted or monosubstituted ligands (*i.e.*,  $\text{Cu}(\text{GTS})$ ,  $\text{Cu}(\text{PTS})$ , or  $\text{Cu}(\text{PTSM})$ ), demonstrated comparable anti-cancer activity in comparison to their corresponding free ligands (*i.e.*, GTS, PTS and PTSM, respectively; Table 2).

In contrast, the  $\text{Cu}^{\text{II}}$  complexes of the disubstituted ligands (*i.e.*,  $\text{Cu}(\text{ATS})$ ,  $\text{Cu}(\text{ATSM})$ ,  $\text{Cu}(\text{CTS})$ ,  $\text{Cu}(\text{CTSM})$ ,  $\text{Cu}(\text{DTS})$ ,  $\text{Cu}(\text{DTSM})$ ,  $\text{Cu}(\text{CyTS})$  and  $\text{Cu}(\text{CyTSM})$ ), displayed significantly ( $p < 0.01$ ) increased anti-proliferative activity ( $\text{IC}_{50}$ : 0.25–2.07  $\mu\text{M}$ ) compared to their corresponding free ligands (Table 2). In fact,  $\text{Cu}$  complexation resulted in a greater than a 6-fold increase in anti-cancer activity. All  $\text{Cu}$  complexes of the disubstituted ligands had significantly ( $p < 0.01$ ) greater anti-proliferative activity relative to DFO (Table 2). Excluding the three

**Table 2**  
 $\text{IC}_{50}$  ( $\mu\text{M}$ ) values of bis(thiosemicarbazone) chelators and their  $\text{Cu}$  complexes at inhibiting the growth of SK-N-MC neuroepithelioma cells and mortal MRC-5 fibroblasts as determined by the MTT assay after a 72 h/37 °C incubation. Results are mean  $\pm$  SD (3 experiments). The  $p$  values were determined using Student's  $t$ -test and compare the activity of the ligand or  $\text{Cu}$  complex in normal and neoplastic cells. NS; not significant.

Ligand	SK-N-MC $\text{IC}_{50}$ ( $\mu\text{M}$ )		MRC-5 $\text{IC}_{50}$ ( $\mu\text{M}$ )		$p$ value		Therapeutic Index	
	Ligand	$\text{Cu}^{\text{II}}(\text{L})$	Ligand	$\text{Cu}^{\text{II}}(\text{L})$	Ligand	$\text{Cu}^{\text{II}}(\text{L})$	Ligand	$\text{Cu}^{\text{II}}(\text{L})$
<i>Controls</i>								
DFO	22.7 $\pm$ 1.6	–	>12.5	–	–	–	–	–
Dp44mT	0.004 $\pm$ 0.001	0.004 $\pm$ 0.001	2.19 $\pm$ 0.07	–	–	–	–	–
3-AP	0.36 $\pm$ 0.03	–	>12.5	–	–	–	–	–
<i>Unsubstituted/monosubstituted</i>								
GTS	0.021 $\pm$ 0.002	0.016 $\pm$ 0.005	8.12 $\pm$ 0.48	0.30 $\pm$ 0.04	$p < 0.01$	$p < 0.05$	387	19
GTSM	0.020 $\pm$ 0.004	0.009 $\pm$ 0.001	6.15 $\pm$ 0.66	0.27 $\pm$ 0.05	$p < 0.01$	$p < 0.05$	308	30
PTS	0.017 $\pm$ 0.003	0.012 $\pm$ 0.001	4.73 $\pm$ 0.75	0.44 $\pm$ 0.05	$p < 0.01$	$p < 0.05$	278	37
PTSM	0.017 $\pm$ 0.003	0.016 $\pm$ 0.001	4.91 $\pm$ 0.74	0.65 $\pm$ 0.08	$p < 0.01$	$p < 0.05$	289	41
<i>Disubstituted</i>								
ATS	>12.5	0.68 $\pm$ 0.13	>12.5	2.60 $\pm$ 0.30	–	$p < 0.05$	–	4
ATSM	>12.5	0.46 $\pm$ 0.17	>12.5	2.13 $\pm$ 0.11	–	$p < 0.05$	–	5
CTS	>12.5	0.25 $\pm$ 0.04	>12.5	1.27 $\pm$ 0.22	–	$p < 0.05$	–	5
CTSM	11.2 $\pm$ 0.82	0.76 $\pm$ 0.04	>12.5	2.09 $\pm$ 0.12	–	$p < 0.05$	>1.1	3
DTS	>12.5	0.51 $\pm$ 0.04	>12.5	1.56 $\pm$ 0.21	–	$p < 0.05$	–	3
DTSM	>12.5	1.83 $\pm$ 0.08	>12.5	3.46 $\pm$ 0.23	–	$p < 0.05$	–	2
CyTS	>12.5	1.56 $\pm$ 0.13	>12.5	3.74 $\pm$ 0.28	–	$p < 0.05$	–	2
CyTSM	>12.5	2.07 $\pm$ 0.23	>12.5	4.79 $\pm$ 0.40	–	$p < 0.05$	–	2

least active complexes, (Cu(DTSM), Cu(CyTS) and Cu(CyTSM)), all other Cu complexes of the disubstituted compounds demonstrated comparable anti-proliferative activity to the ligand, 3-AP ( $IC_{50}$ :  $0.36 \pm 0.03 \mu\text{M}$ ; Table 2).

In summary, Cu complexation greatly enhanced the anti-proliferative activity of disubstituted ligands. On the other hand, the anti-cancer effects of the Cu complexes of the unsubstituted or monosubstituted ligands were either enhanced or comparable to the free ligand. These findings suggest that Cu complexation by bis(thiosemicarbazones) plays a critical role in their anti-proliferative activity. Additionally, examining the correlation between anti-proliferative activity of the Cu complexes and their  $Cu^{II/I}$  redox potentials ( $R^2 = 0.75174$ ; Fig. 2B), demonstrated the existence of two groups, namely: (1) the unsubstituted and monosubstituted group with high anti-proliferative activity and  $Cu^{II/I}$  redox potentials clustered between approximately  $-0.4$  and  $-0.5$  V (red symbols; Fig. 2B); and (2) the disubstituted group, which demonstrated more negative  $Cu^{II/I}$  redox potentials and decreased anti-proliferative efficacy (green symbols; Fig. 2B).

### 3.3.3. Anti-proliferative activity against mortal cells

For a compound to be considered as a possible anti-tumor agent, it must exhibit potent anti-proliferative activity against neoplastic cells, and not markedly affect the proliferation of normal cells. To determine whether these compounds exhibited selectivity towards neoplastic cells, their effect on the proliferation of mortal MRC-5 fibroblasts was assessed (Table 2). Their selectivity was measured using a calculated *in vitro* therapeutic index (Table 2). This parameter represents the ratio of the  $IC_{50}$  values of normal versus neoplastic cells (*i.e.*,  $IC_{50}$  MRC-5/ $IC_{50}$  SK-N-MC; Table 2), with higher values representing greater selectivity against cancer cells.

The unsubstituted or monosubstituted ligands, GTS, GTSM, PTS and PTSM, were significantly ( $p < 0.01$ ) more effective in neoplastic cells than normal MRC-5 fibroblasts, suggesting an appreciable therapeutic index (Table 2). In fact, these ligands displayed  $IC_{50}$  values between 4.73 and 8.12  $\mu\text{M}$  in MRC-5 cells, with therapeutic indices ranging from 278 to 387 (Table 2). In contrast, therapeutic indices of the disubstituted ligands could not be determined, or were  $> 1.1$  (*i.e.*, for CTSM), due to their low anti-proliferative activity against both SK-N-MC and MRC-5 cells.

Pre-complexation of the bis(thiosemicarbazone) ligands with Cu resulted in an increase of anti-proliferative activity in MRC-5 cells relative to the ligands alone (Table 2). This corresponded to a 2.6–27-fold increase in anti-proliferative activity against MRC5 cells upon Cu complexation. Importantly, the anti-proliferative efficacy of the  $Cu^{II}$  bis(thiosemicarbazone) complexes were significantly ( $p < 0.05$ ) decreased in normal MRC-5 cells relative to neoplastic SK-N-MC cells. The Cu complexes of GTS, GTSM, PTS and PTSM displayed appreciable therapeutic indices, ranging between 19 and 41, while the Cu complexes of the disubstituted ligands were less selective, leading to therapeutic indices between 2 and 5 (Table 2).

Collectively, the disubstituted ligands and their Cu complexes were not particularly selective. In contrast, the unsubstituted or monosubstituted ligands and to a lesser extent their Cu complexes possessed very high selectivity owing to their potent anti-proliferative activity against neoplastic cells. Thus, GTS, GTSM, PTS and PTSM and their Cu complexes have appreciable therapeutic indices in targeting cancer cells over normal cells and show promise as potential anti-cancer agents.

### 3.3.4. Bis(thiosemicarbazone)-mediated $^{64}\text{Cu}$ Efflux from cells prelabeled with $^{64}\text{Cu}$

To assess the role of Cu chelation in the anti-neoplastic activity of these bis(thiosemicarbazone) analogs, their ability to mobilize cellular  $^{64}\text{Cu}$  from pre-labeled SK-N-MC cells was assessed (Fig. 3A). Briefly, cells were prelabeled with  $^{64}\text{Cu}$  for 1 h/37 °C, washed, and then

reincubated with medium (control) or medium containing the chelators (25  $\mu\text{M}$ ) for 1 h/37 °C. The efflux of  $^{64}\text{Cu}$  into the medium and the levels of  $^{64}\text{Cu}$  remaining in the cells were then assessed. The release of  $^{64}\text{Cu}$  mediated by the bis(thiosemicarbazone) ligands was compared to Dp44mT and the well characterized Cu chelators, TM (Fig. 1A), and neocuproine (Neo; Fig. 1A) [26].

The three controls, TM, Neo and Dp44mT all significantly ( $p < 0.001$ –0.01) reduced cellular  $^{64}\text{Cu}$  release to  $55 \pm 6\%$ ,  $11 \pm 2\%$  and  $59 \pm 7\%$  of the control, respectively (Fig. 3A). Similar results demonstrating the ability of Dp44mT and TM to inhibit  $^{64}\text{Cu}$  release from SK-N-MC cells has been reported previously [26]. The unsubstituted or monosubstituted bis(thiosemicarbazone) ligands (*i.e.*, GTS, GTSM, PTS and PTSM) also led to significantly ( $p < 0.001$ ) decreased cellular  $^{64}\text{Cu}$  release relative to control medium (control) alone, reducing it to 16–36% of the control (Fig. 3A). The cellular release of  $^{64}\text{Cu}$  mediated by GTS ( $16 \pm 0.5\%$ ) and GTSM ( $20 \pm 1\%$ ) was similar to the Cu chelator, Neo, but significantly ( $p < 0.01$ ) less than TM or Dp44mT. In contrast, three of the disubstituted bis(thiosemicarbazone) compounds (*i.e.*, CTSM, DTSM and CyTSM) were significantly ( $p < 0.01$ ) more effective at mediating  $^{64}\text{Cu}$  mobilization relative to the control medium, increasing  $^{64}\text{Cu}$  release to 146–161% of the control (Fig. 3A). In contrast, their terminal amine ( $R_3$ ) unsubstituted counterparts (*i.e.*, CTS, DTS and CyTS) and the diacetyl bis(thiosemicarbazone) ligands (*i.e.*, ATS and ATSM) did not significantly ( $p > 0.05$ ) alter  $^{64}\text{Cu}$  release relative to the control (Fig. 3A).

Generally, the unsubstituted or monosubstituted chelators possessing high anti-proliferative activity (*i.e.*, GTS, GTSM, PTS and PTSM; Table 2) demonstrated a decrease in intracellular  $^{64}\text{Cu}$  release relative to the control (*i.e.*, an accumulation of intracellular  $^{64}\text{Cu}$ ). In contrast, the disubstituted ligands with poor anti-proliferative activity (Table 2) demonstrated comparable or enhanced  $^{64}\text{Cu}$  release relative to the control in SK-N-MC cells (Fig. 3A). This observation is in agreement with a study demonstrating the cellular accumulation of  $^{64}\text{Cu}$  complexes of unsubstituted or monosubstituted bis(thiosemicarbazones), such as GTS, GTSM, PTS and PTSM, and the release of  $^{64}\text{Cu}$  complexes of disubstituted ligands, including ATS and ATSM, using mouse mammary EMT6 tumor cells [20].

Plotting  $^{64}\text{Cu}$  release from cells against their one electron  $Cu^{II/I}$  redox potentials yielded a correlation ( $R^2 = 0.7861$ ) and demonstrated the existence of 2 groups, namely: (1) the unsubstituted and monosubstituted bis(thiosemicarbazones) (green; Fig. 3B); and (2) the disubstituted bis(thiosemicarbazones) (red; Fig. 3B). The enhanced lipophilicity of the terminal amine ( $R_3$ ) methylated disubstituted analogs (*i.e.*, CTSM, DTSM and CyTSM;  $\text{Log } P_{\text{calc}}$  2.34–2.78; Table 1) may have facilitated the passive diffusion of the ligand and their complexes through the plasma membrane lipid bilayer relative to their terminal amine unsubstituted analogs (*i.e.*, CTS, DTS and CyTS;  $\text{Log } P_{\text{calc}}$  1.34–2.15; Table 1), resulting in enhanced cellular  $^{64}\text{Cu}$  release (Fig. 3A). In fact, a plot of the  $^{64}\text{Cu}$  release vs.  $\text{Log } P_{\text{calc}}$  values yielded a correlation coefficient ( $R^2$ ) of 0.7536 (Fig. 3C). Collectively, these results suggest the importance of the lipophilicity of these agents and also their  $Cu^{II/I}$  redox potentials on their ability to mobilize cellular  $^{64}\text{Cu}$ . Indeed, the ligands that formed Cu complexes with more biologically accessible reduction potentials and that were relatively more hydrophilic (*i.e.*, GTS, GTSM, PTS and PTSM;  $\text{Log } P_{\text{calc}}$  0.45–1.45; Table 1), led to less cellular  $^{64}\text{Cu}$  release (Fig. 3A) and potent anti-proliferative activity (Table 2).

### 3.3.5. Release of $^{64}\text{Cu}$ from cells prelabeled with the $^{64}\text{Cu}$ [bis(thiosemicarbazone)] complexes

As a comparison to cellular labeling using  $^{64}\text{Cu}$  alone (Fig. 3A), and to further assess the ability of the bis(thiosemicarbazone) ligands to mobilize intracellular  $^{64}\text{Cu}$ , SK-N-MC cells were prelabeled with bis(thiosemicarbazone)  $^{64}\text{Cu}$ -complexes (1:1) and the release examined (Fig. 3D). Briefly, in these studies, SK-N-MC cells were incubated for 1 h/37 °C with the preformed  $^{64}\text{Cu}$ [bis(thiosemicarbazone)] complexes (25  $\mu\text{M}$ ). Then the cells were washed and re-incubated with

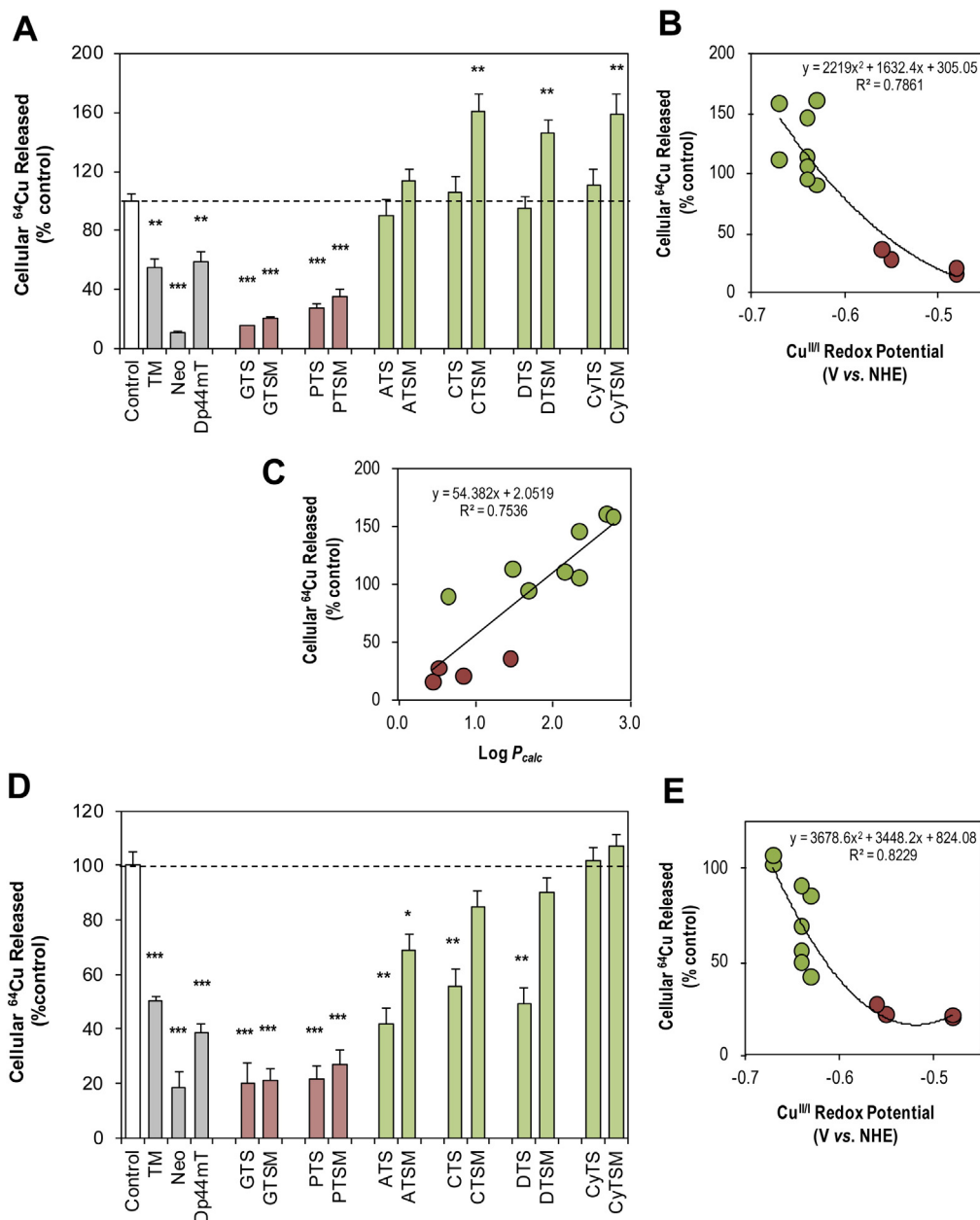


**Fig. 3.** The effect of bis(thiosemicarbazone) series ligands on: (A) <sup>64</sup>Cu cellular mobilization from SK-N-MC neuroepithelioma cells prelabeled with <sup>64</sup>Cu; (B) the relationship between <sup>64</sup>Cu cellular mobilization and Cu<sup>II</sup> redox potential; and (C) the relationship between <sup>64</sup>Cu cellular mobilization and lipophilicity (Log P<sub>calc</sub>). The effect of bis(thiosemicarbazone) series ligands on: (D) release of <sup>64</sup>Cu from SK-N-MC cells prelabeled with bis(thiosemicarbazone) <sup>64</sup>Cu-complexes formed in situ; and (E) the relationship between <sup>64</sup>Cu cellular release in (D) and Cu<sup>II</sup> redox potentials. Results are mean ± SD (3 experiments). \*, versus control,  $p < 0.05$ ; \*\*, versus control,  $p < 0.01$ ; \*\*\*, versus control,  $p < 0.001$ .

media for 1 h/37 °C. The percentage of <sup>64</sup>Cu released from cells was then quantified, and expressed as a percentage of that found for cells incubated with medium alone (i.e., control). The release of <sup>64</sup>Cu from cells after labeling with the <sup>64</sup>Cu[bis(thiosemicarbazone)] complexes were compared to the preformed <sup>64</sup>Cu complexes of Dp44mT, TM and Neo, as relative controls (Fig. 3D).

The preformed <sup>64</sup>Cu complexes of TM, Neo and Dp44mT, resulted in significantly ( $p < 0.001$ ) decreased <sup>64</sup>Cu release that was 50%, 19% and 39% of the control, respectively (Fig. 3D). Cells incubated with the <sup>64</sup>Cu complexes of GTS, GTSM, PTS and PTSM all demonstrated significantly ( $p < 0.001$ ) decreased levels of <sup>64</sup>Cu release (20–27%) relative to the control, and this was also significantly ( $p < 0.01$ – $0.05$ ) less than the release of <sup>64</sup>Cu complexes of TM and Dp44mT (Fig. 3D). In fact, the <sup>64</sup>Cu complexes of GTS, GTSM and PTS mediated comparable levels of cellular <sup>64</sup>Cu release to that of <sup>64</sup>Cu-Neo (Fig. 3D). Additionally, the <sup>64</sup>Cu complexes of all disubstituted ligands, which previously

demonstrated poor anti-proliferative activity (Table 2), showed significantly ( $p < 0.05$ ) increased <sup>64</sup>Cu release compared to the <sup>64</sup>Cu complexes of the unsubstituted or monosubstituted ligands (Fig. 3D) that displayed potent anti-cancer effects (Table 2). However, the <sup>64</sup>Cu complexes of the disubstituted ligands, ATS, ATSM, CTS and DTS, demonstrated significantly ( $p < 0.01$ – $0.05$ ) decreased <sup>64</sup>Cu release compared to the control. The <sup>64</sup>Cu complexes of the remaining disubstituted ligands, namely, CTSM, DTSM, CyTS and CyTSM, mediated comparable levels of <sup>64</sup>Cu release relative to the control (Fig. 3D). Similarly to the cellular <sup>64</sup>Cu mobilization results above (Fig. 3A,B), a correlation ( $R^2 = 0.8229$ ) was observed between <sup>64</sup>Cu release (Fig. 3D) and their Cu<sup>II</sup> redox potentials (Fig. 3E). Hence, irrespective of cellular prelabeling with <sup>64</sup>Cu or <sup>64</sup>Cu-bis(thiosemicarbazone) complexes, a similar trend in <sup>64</sup>Cu release was observed with the unsubstituted/monosubstituted and disubstituted analogs, with again these two groups demonstrating distinctly different activity.

Previous structure–activity relationship studies have proposed that bio-reduction of the complexed  $\text{Cu}^{\text{II}}$  to  $\text{Cu}^{\text{I}}$  by intracellular reductants was critical for their cellular accumulation [38]. Upon reduction, the formed  $\text{Cu}^{\text{I}}$  complex (e.g.,  $\text{Cu}(\text{GTSM})^-$ ) was trapped within the cell, owing to its negative charge and it was suggested that the fate of the  $\text{Cu}^{\text{I}}$  complex was dependent on its ability to be re-oxidized [37]. For example, the  $\text{Cu}^{\text{I}}$  complexes with more negative  $\text{Cu}^{\text{II/I}}$  redox potentials, such as  $\text{Cu}(\text{ATSM})^-$ , were readily oxidized to regenerate the neutral  $\text{Cu}^{\text{II}}$  complex (e.g.,  $\text{Cu}^{\text{II}}(\text{ATSM})$ ), which can diffuse out of the cell [37]. In contrast,  $\text{Cu}^{\text{I}}$  complexes with more positive  $\text{Cu}^{\text{II/I}}$  redox potentials, such as  $\text{Cu}(\text{GTSM})^-$ , were not readily oxidized, resulting in the intracellular trapping of  $\text{Cu}$  [20]. Hence, the observed  $^{64}\text{Cu}$  accumulation by complexes with more positive (i.e., more readily reduced)  $\text{Cu}^{\text{II/I}}$  redox potentials (e.g.,  $\text{Cu}(\text{GTSM})$ ) is in agreement with the proposed model of redox potential-dependent intracellular reductive trapping [20].

### 3.3.6. Anti-neoplastic activity of potent bis(thiosemicarbazones) is mediated by copper complexation

To further investigate the role of Cu chelation in the anti-neoplastic activity of the bis(thiosemicarbazones), the ability of the well-known Cu chelator, TM (Fig. 1A) [62], to modulate the anti-proliferative activity of the bis(thiosemicarbazones) and their Cu complexes was examined. Notably, TM is a Cu specific chelator with low toxicity that forms Cu complexes [62], and markedly decreases the cytotoxicity of other potent thiosemicarbazones [26]. In these studies, we assessed the effect of TM ( $5\ \mu\text{M}$ ) on the anti-proliferative activity of the ligands and Cu complexes

(Fig. 4A and B; Table 3) of two highly potent unsubstituted or monosubstituted bis(thiosemicarbazones), namely GTSM and PTSM, relative to a disubstituted ligand with low anti-proliferative efficacy, ATSM (Table 2).

Incubation of SK-N-MC cells with TM resulted in an  $\text{IC}_{50}$  of  $>6.25\ \mu\text{M}$  (Table 3). Thus, TM alone at  $5\ \mu\text{M}$  did not result in any significant cytotoxicity. Interestingly, in the presence of TM, the anti-proliferative activity of GTSM or PTSM was markedly decreased, leading to an increase in the  $\text{IC}_{50}$  from  $0.017\text{--}0.019\ \mu\text{M}$  to  $>6.25\ \mu\text{M}$  (Fig. 4A, Table 3). This alteration represented a  $>329$ -fold decrease in the anti-proliferative activity of GTSM and PTSM. In contrast, the anti-proliferative activity of ATSM ( $\text{IC}_{50} > 6.25\ \mu\text{M}$ ) was greatly enhanced in the presence of TM, leading to an  $\text{IC}_{50}$  value of  $0.07\ \mu\text{M}$  (Table 3). This represented a  $>89$ -fold increase in the anti-proliferative activity of ATSM (Fig. 4A; Table 3). This latter finding suggested that the addition of TM led to a synergistic interaction with ATSM in regards to cytotoxicity via an unknown mechanism.

Co-incubation of TM with the pre-formed Cu complexes of GTSM or PTSM also resulted in a marked and significant ( $p < 0.01$ ) decrease in their anti-proliferative activity from  $0.037\text{--}0.039\ \mu\text{M}$  to  $0.19\ \mu\text{M}$ , which represented a 4.9 to 5.1-fold increase in their  $\text{IC}_{50}$  values (Fig. 4B; Table 3). A smaller, but significant ( $p < 0.05$ ), 1.6-fold decrease in anti-proliferative activity was also observed for  $\text{Cu}(\text{ATSM})$  upon co-incubation with TM viz., from  $0.31\ \mu\text{M}$  to  $0.50\ \mu\text{M}$  (Table 3).

These data suggest the importance of chelatable Cu in the anti-proliferative activity of the GTSM and PTSM ligands. It can be speculated

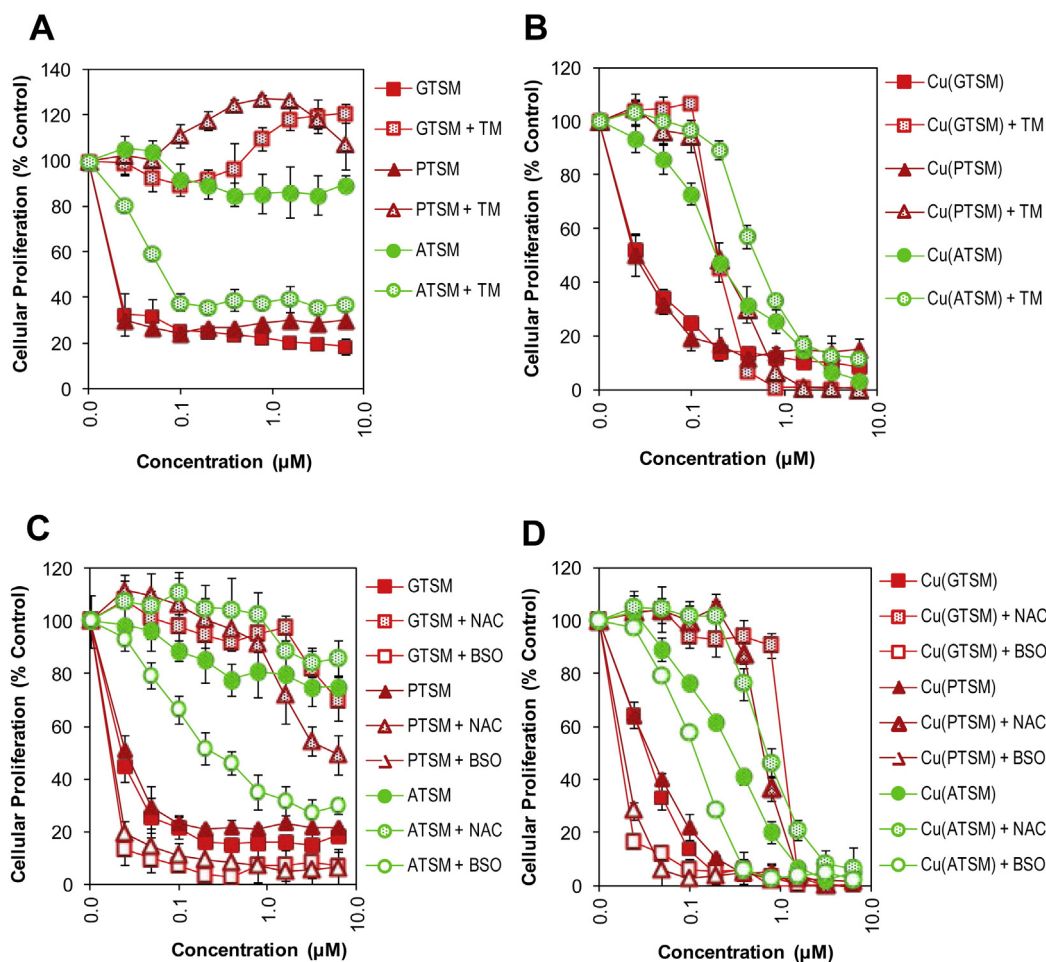


**Fig. 4.** Anti-proliferative activity of: (A) bis(thiosemicarbazone) ligands, GTSM, PTSM and ATSM, and (B) their copper complexes,  $\text{Cu}(\text{GTSM})$ ,  $\text{Cu}(\text{PTSM})$  and  $\text{Cu}(\text{ATSM})$ , with or without a 10 min/ $37\ ^\circ\text{C}$  pre-incubation with the non-toxic copper chelator, TM ( $5\ \mu\text{M}$ ). Anti-proliferative activity of the: (C) bis(thiosemicarbazone) ligands, GTSM, PTSM and ATSM, and (D) their copper complexes,  $\text{Cu}(\text{GTSM})$ ,  $\text{Cu}(\text{PTSM})$  and  $\text{Cu}(\text{ATSM})$ , with or without a pre-incubation with NAC ( $5\ \text{mM}$ ) for 10 min or BSO ( $100\ \mu\text{M}$ ) for 16 h/ $37\ ^\circ\text{C}$ . Results are mean  $\pm$  SD (3 experiments).

**Table 3**  
IC<sub>50</sub> (μM) values of bis(thiosemicarbazone) chelators and their Cu complexes at inhibiting the growth of SK-N-MC neuroepithelioma cells in the presence of TM, NAC or BSO. Results are mean ± SD (3 experiments). NS; not significant.

Compound	IC <sub>50</sub> (μM)	+ TM		+ NAC		+ BSO	
		IC <sub>50</sub> (μM)	p value	IC <sub>50</sub> (μM)	p value	IC <sub>50</sub> (μM)	p value
TM	>6.25						
GTSM	0.019 ± 0.004	>6.25	–	>6.25	–	0.014 ± 0.001	NS
PTSM	0.017 ± 0.003	>6.25	–	>6.25	–	0.014 ± 0.002	NS
ATSM	>6.25	0.07 ± 0.005	–	>6.25	–	0.26 ± 0.05	–
Cu(GTSM)	0.037 ± 0.005	0.19 ± 0.01	p < 0.01	1.14 ± 0.03	p < 0.01	0.015 ± 0.001	p < 0.05
Cu(PTSM)	0.039 ± 0.002	0.19 ± 0.01	p < 0.01	0.68 ± 0.03	p < 0.01	0.020 ± 0.001	p < 0.05
Cu(ATSM)	0.31 ± 0.027	0.50 ± 0.04	p < 0.05	0.74 ± 0.07	p < 0.05	0.12 ± 0.02	p < 0.05

that TM may not only be able to compete with GTSM and PTSM for cellular Cu, but may also remove Cu from their pre-formed Cu complexes to inhibit their anti-proliferative activity. Thus, Cu chelation by these bis(thiosemicarbazones) is an important mechanism of their anti-cancer activity.

### 3.3.7. Anti-proliferative activity is modulated by intracellular glutathione levels

The electrochemical studies reported in Table 1 illustrate the potential ability of Cu complexes of bis(thiosemicarbazones) to cycle between the oxidized (Cu<sup>II</sup>) and reduced (Cu<sup>I</sup>) states at potentials accessible to biological oxidants and reductants. In fact, the complexes with the most positive redox potentials (*i.e.*, Cu(GTS), Cu(GTSM), Cu(PTS) and Cu(PTSM); Table 1) also possessed the highest anti-proliferative activity (Table 2), and resulted in decreased <sup>64</sup>Cu release from cells (Fig. 3). The presence of excess cellular Cu (both endogenous and as exogenous Cu complexes) has previously been shown to be a potent oxidant, resulting in the generation of ROS in cells [11,26]. Thus, we assessed whether the anti-proliferative activity of the bis(thiosemicarbazones) and their Cu complexes was related to their ability to generate oxidative stress. To examine this, SK-N-MC cells were incubated for 72 h/37 °C with increasing concentrations of GTSM, PTSM and ATSM, or their pre-formed Cu complexes either: (1) in the presence of NAC (5 mM); or (2) with a 16 h/37 °C pre-incubation with BSO (100 μM) or media alone (Fig. 4C and D). Notably, NAC is a well characterized anti-oxidant [54,55] and is a precursor of glutathione (GSH), that has been shown to prevent the redox-induced cytotoxicity of thiosemicarbazones (*e.g.*, Dp44mT) and their Cu complexes [26]. Conversely, BSO has been demonstrated to increase the oxidative stress of Dp44mT by reducing cellular levels of GSH through the inhibition of γ-glutamylcysteine synthetase, the enzyme required for the first step of GSH synthesis [26,70].

The addition of the anti-oxidant, NAC, led to a marked and significant (*p* < 0.01) decrease in the anti-proliferative activity of GTSM and PTSM, increasing their IC<sub>50</sub> values from 0.017–0.019 μM, respectively, to >6.25 μM (Fig. 4C, Table 3). This represented a >329-fold decrease in the anti-proliferative activity of GTSM and PTSM in the presence of NAC. The IC<sub>50</sub> of ATSM was not achieved in the absence or presence of NAC (>6.25 μM; Table 3), although NAC slightly decreased the anti-proliferative efficacy of ATSM relative to ATSM alone (Fig. 4C). A 16 h/37 °C pre-incubation of SK-N-MC cells with BSO prior to the addition of GTSM or PTSM resulted in a slight, but not significant (*p* > 0.05), increase in their anti-proliferative activity (Fig. 4C; Table 3). However, BSO pre-incubation resulted in a marked >24-fold decrease in the IC<sub>50</sub> of ATSM relative to ATSM alone (*i.e.*, a decrease in IC<sub>50</sub> from >6.25 μM to 0.26 μM; Table 3; Fig. 4C).

Incubation with NAC also had a pronounced effect on decreasing the anti-proliferative activity of the Cu[bis(thiosemicarbazone)] complexes (Fig. 4D, Table 3). In fact, incubation of the Cu(GTSM), Cu(PTSM) and Cu(ATSM) complexes with NAC demonstrated a significant (*p* < 0.01–0.05) decrease in their anti-proliferative activity, resulting in a 31-, 17- and 2.4-fold increase in their IC<sub>50</sub> values, respectively (Table 3). Pre-incubation with BSO to deplete cellular GSH led to an increase in anti-proliferative activity of all the Cu[bis(thiosemicarbazone)] complexes

(Fig. 4D; Table 3). In fact, the anti-proliferative activity of Cu(GTSM), Cu(PTSM) and Cu(ATSM), were significantly (*p* < 0.05) enhanced in the presence of BSO, with IC<sub>50</sub> values decreasing from 0.037–0.31 μM to 0.015–0.12 μM (Fig. 4D, Table 3). This corresponded to a 2–2.6-fold increase in anti-proliferative activity.

In summary, augmentation of GSH levels through incubation of cells with the anti-oxidant, NAC, resulted in a decrease in the anti-proliferative activity of the bis(thiosemicarbazones). This result was observed for both the free ligands and pre-formed Cu complexes and was most prominent for the more potent ligands, GTSM and PTSM. In addition, attenuation of the ability of the cell to manage redox stress by depleting cellular GSH with BSO potentiated the anti-proliferative activity of the free ligands and their Cu complexes. These findings suggest that bis(thiosemicarbazones) and their Cu complexes mediate their anti-proliferative activity through the promotion of ROS generation.

### 3.3.8. Copper complexation is required for bis(thiosemicarbazone)-mediated ROS generation

To further examine the relevance of ROS generation on the anti-proliferative activity of bis(thiosemicarbazones), and their Cu complexes, we examined their ability to catalyze the oxidation of the non-fluorescent redox probe, H<sub>2</sub>DCF-DA, to its fluorescent counterpart, DCF, using SK-N-MC cells (Fig. 5). Importantly, DCF is a well-characterized probe for assessing intracellular redox stress [22,57,71]. The SK-N-MC cells were incubated with GTSM (2 or 25 μM) or Cu(GTSM) (5 μM) for 1 h/37 °C with or without a 10 min/37 °C pre-incubation with CuCl<sub>2</sub> (5 μM) and/or TM (5 μM). The concentrations of chelators and complexes chosen represent the highest concentrations that could be used without inducing excessive toxicity. For example, pre-incubation of cells with CuCl<sub>2</sub> (5 μM), prior to incubation with GTSM (25 μM), resulted in loss of cell membrane integrity and the DCF signal (data not shown). Thus, after pre-incubation with CuCl<sub>2</sub> (5 μM), cells were incubated with GTSM (2 μM) to ensure cellular viability. In parallel studies, hydrogen peroxide (H<sub>2</sub>O<sub>2</sub>; 50 μM) was used as a positive control [22]. The results were assessed by flow cytometry (Fig. 5A, B) and were quantified and expressed as a percentage of the control (Fig. 5C).

The positive control, H<sub>2</sub>O<sub>2</sub>, led to a significant (*p* < 0.01) increase in DCF fluorescence to 294 ± 17% of the control (Fig. 5C). In contrast, pre-incubation of cells with CuCl<sub>2</sub> (5 μM) alone did not significantly (*p* > 0.05) alter DCF fluorescence (94 ± 7%) relative to control cells (Fig. 5C). Incubation of cells with GTSM (25 μM) alone mediated a small, but significant (*p* < 0.05), increase in intracellular DCF fluorescence to 112 ± 10% of the control (Fig. 5C).

Incubation with GTSM (2 μM) after CuCl<sub>2</sub> (5 μM) pre-incubation led to an increase in DCF fluorescence intensity, resulting in the peak being shifted to the right relative to control cells (red shading; Fig. 5A). Quantification of these results demonstrated a substantial and significant (*p* < 0.01) increase in DCF fluorescence to 188 ± 16% of control (Fig. 5C). Moreover, DCF fluorescence from SK-N-MC cells incubated with GTSM (2 μM) after preincubation with CuCl<sub>2</sub> (5 μM) was also significantly (*p* < 0.01) increased relative to incubation with the GTSM

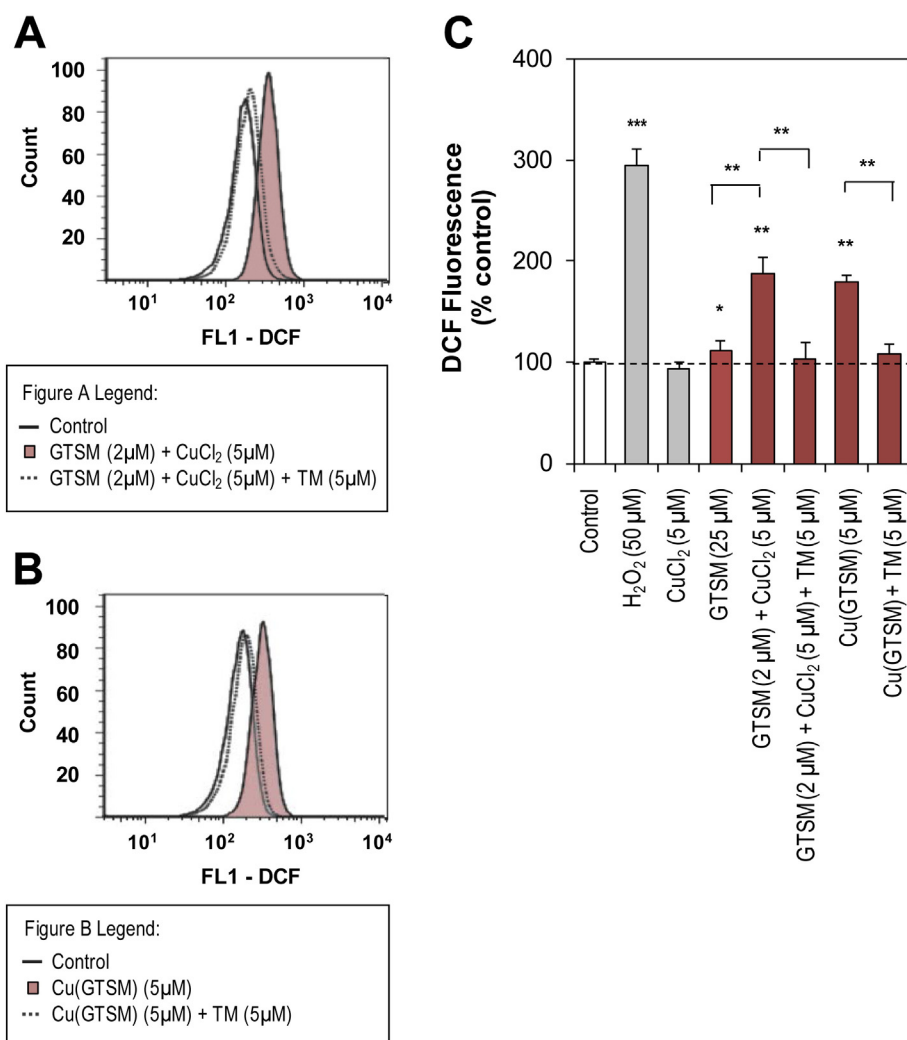


**Fig. 5.** Intracellular redox stress was measured using DCF in SK-N-MC cells and assessed with flow cytometry. Cells were incubated with medium alone (control) or: (A) GTSM with a 10 min/37 °C pre-incubation with Cu (5 μM) and/or TM (5 μM); (B) Cu(GTSM), with or without a 10 min/37 °C pre-incubation with TM (5 μM); (C) Geometric mean of obtained peaks. Results are mean ± SD (3 experiments). \*, versus control,  $p < 0.05$ ; \*\*, versus control,  $p < 0.01$ ; \*\*\*, versus control,  $p < 0.001$ .

ligand (25 μM) alone, despite the greater than ten-fold higher concentration of the ligand. To investigate the effect of Cu chelation on the ability of the bis(thiosemicarbazones) to mediate ROS generation, cells were also pre-incubated with TM. Pre-incubation of cells with TM and Cu led to a significant ( $p < 0.01$ ) decrease in GTSM (2 μM) and Cu (5 μM)-mediated DCF fluorescence to  $105 \pm 10\%$  of the control (Fig. 5C).

The pre-formed Cu complex, Cu(GTSM), was also able to mediate a significant ( $p < 0.01$ ) increase in DCF fluorescence which was demonstrated by a right shift in DCF fluorescence intensity (red shading; Fig. 5B) and an increased in DCF fluorescence to  $174 \pm 6\%$  of the control (Fig. 5C). Importantly, pre-incubation with TM significantly ( $p < 0.01$ ) decreased the Cu(GTSM)-mediated DCF fluorescence to  $107 \pm 16\%$  of the control (Fig. 5C). This observation suggested that TM was able to remove Cu from the pre-formed complex.

Collectively, these results using DCF demonstrate the ability of GTSM and its Cu complex to catalyze the formation of intracellular ROS. Importantly, this effect was reversed in the presence of the Cu chelator, TM, demonstrating the importance of Cu chelation in GTSM-mediated ROS generation.

### 3.3.9. Bis(thiosemicarbazones) target lysosomal integrity

Our previous studies revealed that the lysosome is an important cellular target in the anti-cancer activity of the Cu thiosemicarbazone

complex, Cu<sup>II</sup>(Dp44mT) [26]. This redox active Cu complex was found to accumulate in lysosomes, inducing apoptosis by disrupting lysosome integrity [26]. This mechanism of cell death has not been reported for bis(thiosemicarbazones), and considering the reliance of bis(thiosemicarbazones) anti-proliferative activity on cellular retention of Cu (Fig. 3A, D) and Cu complexation (Figs. 4A, B; 5A–C), we examined whether these agents could also target the lysosome. These studies were initially performed using the lysosomotropic fluorophore, AO (Fig. 6), which becomes concentrated in lysosomes and results in a granular red fluorescence, while AO in the cytosol or nucleus emits a diffuse green fluorescence [26,72,73]. A reduction in granular red fluorescence combined with an increased diffuse cytosolic green fluorescence, indicates relocation of AO from the lysosomes to the cytosol, following changes in lysosomal membrane permeability [58]. To examine the ability of GTSM to affect AO localization, SK-N-MC cells were incubated with GTSM for 1 h/37 °C with or without a 10 min/37 °C pre-incubation with Cu (5 μM). Additionally, these cells were also pre-incubated with TM (5 μM) or NAC (2 mM) for 10 min/37 °C, and/or BSO (100 μM) for 16 h/37 °C, prior to a 1 h incubation with GTSM. The red fluorescence intensity was quantified with image processing and analysis software, ImageJ v1.48 (Fig. 6).

Control SK-N-MC cells showed a granular red fluorescence consistent with AO concentrated in lysosomes (Fig. 6A(a)) [74]. No significant

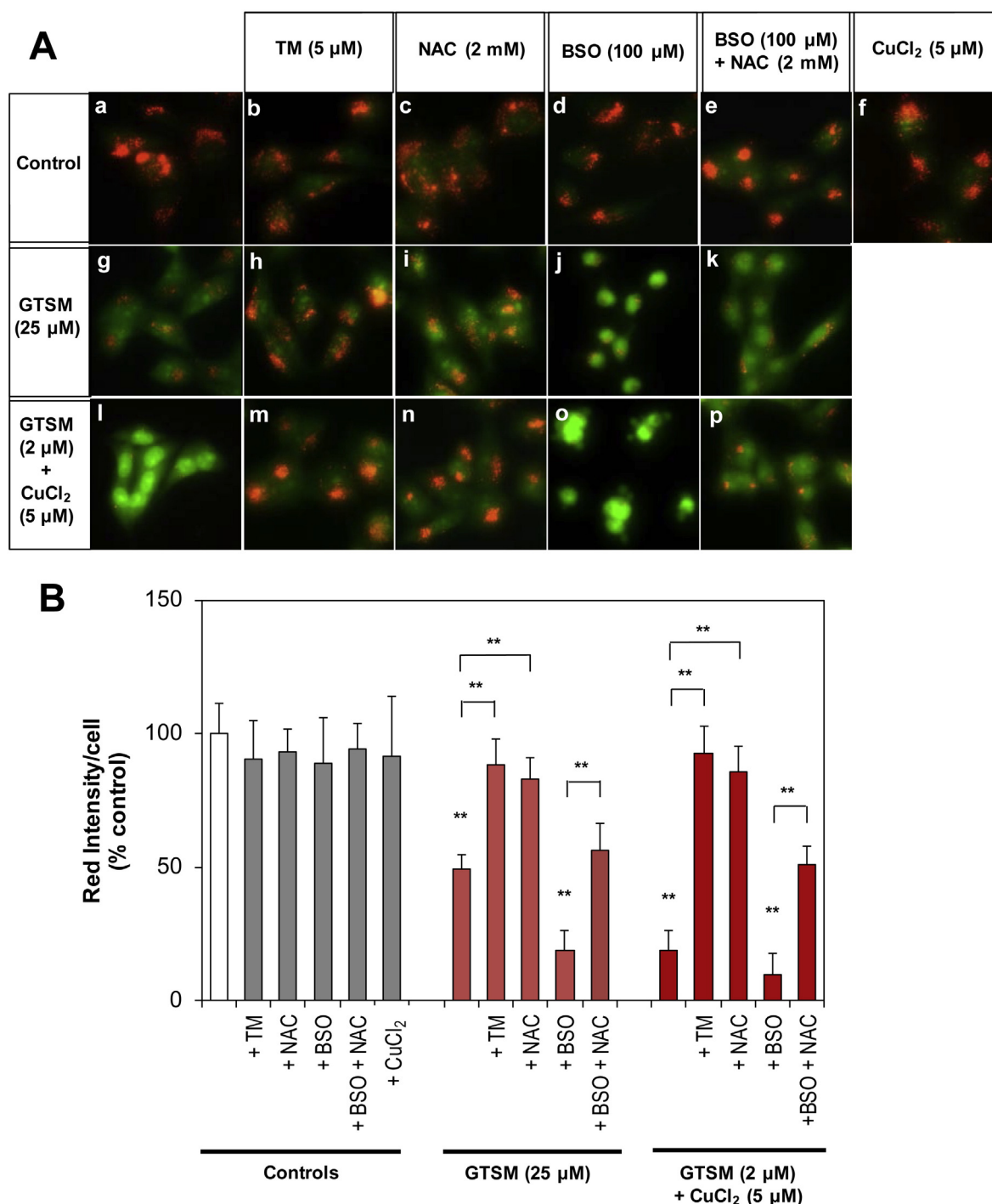


**Fig. 6.** (A) Acridine orange (AO) lysosomal stability study in SK-N-MC cells to assess lysosomal membrane permeabilization (LMP). (A) Cells were incubated with GTSM (2 or 25  $\mu$ M) for 1 h/37  $^{\circ}$ C, with or without a Cu (5  $\mu$ M) pre-incubation for 10 min/37  $^{\circ}$ C, and with pre-incubation with TM (5  $\mu$ M) or NAC (5 mM) over 10 min/37  $^{\circ}$ C; or BSO (100  $\mu$ M) for 16 h/37  $^{\circ}$ C. (B) Quantification of AO (red fluorescence) using the image processing and analysis software, ImageJ v1.48. Results are typical of 3 experiments. \*\*, versus control,  $p < 0.01$ . (For interpretation of the references to color in this figure legend, the reader is referred to the web version of this article.)

( $p > 0.05$ ) alteration in red fluorescence was observed upon incubation of cells with either TM, NAC, BSO, BSO + NAC, or CuCl<sub>2</sub> (Fig. 6A(b)–(f), and 6B). Incubation of cells with GTSM alone resulted in a marked and significant ( $p < 0.01$ ) decrease in red fluorescence to  $49 \pm 3\%$  (Fig. 6A(g), B) relative to the control (Fig. 6A(a), B). This was accompanied by an increase in cytosolic green fluorescence consistent with relocation of AO from the lysosomes to the cytosol, indicating that GTSM caused lysosomal membrane permeabilization (LMP; Fig. 6A(g)).

Upon pre-incubation with the Cu chelator, TM (Fig. 6A(h)), or the anti-oxidant, NAC (Fig. 6A(i)), the ability of GTSM to mediate the relocation of AO to the cytosol was significantly ( $p < 0.01$ ) inhibited relative to GTSM alone (Fig. 6A(g)). In fact, TM or NAC significantly ( $p < 0.01$ ) increased red fluorescence in GTSM-treated cells to 93% and 86% of the control, respectively, and this was comparable to control cells (Fig. 6B). Pre-incubation with BSO (Fig. 6A(j)), prior to the addition of GTSM, led to a significant ( $p < 0.01$ ) decrease in red fluorescence ( $19 \pm 8\%$ ; Fig. 6B) relative to the control (Fig. 6A(a)), or GTSM alone

(Fig. 6A(g)), and resulted in marked changes in cellular morphology (i.e., a clear decrease in cell size denoting possible damage). Co-incubation of cells with GTSM, BSO and NAC (Fig. 6A(k)) resulted in a significant ( $p < 0.01$ ) increase in red fluorescence ( $56 \pm 10\%$ ; Fig. 6B) relative to cells incubated with GTSM and BSO alone (Fig. 6A(j)). Hence, NAC decreased the pronounced effect of BSO and GTSM and led to an increase in cell size, suggesting less toxicity.

Pre-incubation of cells with  $\text{CuCl}_2$  ( $5 \mu\text{M}$ ), prior to the addition of GTSM ( $25 \mu\text{M}$ ; i.e., denoted as GTSM +  $\text{CuCl}_2$ ), led to a complete loss of cells (data not shown) demonstrating the pronounced toxicity of the combination, probably due to enhanced formation of the potentially cytotoxic, Cu–GTSM complex (Table 2). Thus, in these studies, the concentration of GTSM was decreased to  $2 \mu\text{M}$  to obtain viable cells for examination. Despite the lower GTSM concentration, incubation with GTSM +  $\text{CuCl}_2$  resulted in a significant ( $p < 0.01$ ) decrease in red fluorescence ( $19 \pm 5\%$  vs. control; Fig. 6B), and the near disappearance of red granular fluorescence (Fig. 6A(l)). Simultaneous with this decrease in red fluorescence, was an increase in green fluorescence, consistent with the redistribution of AO from lysosomes to the cytosol following the loss of lysosomal integrity (Fig. 6A(l)). Pre-incubation of cells with TM (Fig. 6A(m)) or NAC (Fig. 6A(n)) significantly ( $p < 0.01$ ) increased red fluorescence to  $88 \pm 10\%$  and  $83 \pm 9\%$  of the control, respectively (Fig. 6B). In fact, the level of red fluorescence observed in GTSM +  $\text{CuCl}_2$ -treated cells that received TM or NAC pre-treatment was comparable to the control (Fig. 6A(a)) and there was only minimal redistribution of AO to the cytosol (Fig. 6A(m), (n); Fig. 6B). This observation was consistent with TM or NAC preventing the ability of GTSM +  $\text{CuCl}_2$  in disrupting lysosomal stability.

A 16 h/37 °C pre-incubation of cells with BSO, prior to GTSM and Cu treatment (i.e., GTSM +  $\text{CuCl}_2$  + BSO), led to marked morphological changes consistent with apoptotic budding (Fig. 6A(o)), a characteristic sign of cell death [75]. This effect was accompanied by an almost complete and significant ( $p < 0.01$ ) loss of red fluorescence ( $9 \pm 8\%$ ) relative to the control (Fig. 6B), suggesting extensive LMP [76]. Relative to GTSM +  $\text{CuCl}_2$  + BSO alone (Fig. 6A(o)), the addition of NAC prevented the apoptotic changes (Fig. 6A(p)) and resulted in a significant ( $p < 0.01$ ) increase in granular red fluorescence ( $50 \pm 11\%$ ; Fig. 6B) relative to BSO alone. Collectively, these results demonstrate that GTSM is able to mediate LMP in SK-N-MC cells. This effect can be potentiated by BSO that depletes cells of the anti-oxidant, GSH [70], or prevented by NAC that supplements cellular GSH [55]. Importantly, the effect of GTSM on LMP is potentiated by the addition of Cu and prevented by the non-toxic Cu chelator, TM. Hence, together with the results from Fig. 5, it can be deduced that a redox active GTSM–Cu complex can induce LMP.

To elucidate the mechanisms involved in the selectivity of the bis(thiosemicarbazones) towards neoplastic cells (Table 2), mortal MRC-5 fibroblast cells were compared to SK-N-MC neuroepithelioma cells using the lysosomotropic fluorophore, AO (Fig. 7). As shown in Fig. 6 examining SK-N-MC cells, both SK-N-MC (Fig. 7A(a)) and MRC-5 cells (Fig. 7A(e)) incubated with control medium only (control) showed a granular red fluorescence consistent with AO concentrated in lysosomes. Incubation of SK-N-MC cells (Fig. 7A(b)) or MRC-5 cells (Fig. 7A(f)) with  $\text{CuCl}_2$  alone resulted in no significant ( $p > 0.05$ ) effect relative to the respective controls (Fig. 7A(a) and (e)). Examining SK-N-MC cells, GTSM ( $25 \mu\text{M}$ ) led to a significant ( $p < 0.01$ ) decrease in red fluorescence ( $56 \pm 12\%$ ) relative to the control (Fig. 7A(c) cf. 7A(a); Fig. 7B). In contrast, using mortal MRC5 cells, GTSM ( $25 \mu\text{M}$ ) resulted in a slight, but not significant ( $p > 0.05$ ) increase in red fluorescence to  $146 \pm 32\%$  (Fig. 7A(g)) relative to the control (Fig. 7A(e); Fig. 7B). These results demonstrate that neoplastic SK-N-MC cells were more sensitive to LMP relative to mortal MRC5 cells.

Additionally, co-treatment of SK-N-MC cells with GTSM ( $2 \mu\text{M}$ ) +  $\text{CuCl}_2$  ( $5 \mu\text{M}$ ) led to an almost complete loss of red fluorescence (Fig. 7A(d)) relative to the control (Fig. 7A(a)). This observation corresponded to a marked and significant ( $p < 0.01$ ) decrease in red

fluorescence to  $21 \pm 6\%$  of the control cells (Fig. 7B). In contrast, incubation of MRC-5 cells with GTSM ( $2 \mu\text{M}$ ) +  $\text{CuCl}_2$  ( $5 \mu\text{M}$ ) did not result in a significant ( $p > 0.05$ ) change in red fluorescence ( $137 \pm 6\%$ ; Fig. 7A(h); Fig. 7B) and was comparable to the control (Fig. 7A(e)).

The investigation above in Fig. 7 is consistent with the cellular proliferation studies where the bis(thiosemicarbazones) and their Cu complexes showed selective anti-cancer activity against neoplastic SK-N-MC cells relative to mortal MRC-5 cells (Table 2). Together, these studies suggest that the mechanism of this selectivity of bis(thiosemicarbazones) towards neoplastic cells is related to susceptibility to lysosomal injury. It can be speculated that this could potentially be due to: (1) the greater metabolic turnover in tumor cells relative to mortal cells [11]; (2) enhanced intracellular ROS in cancer cells [15]; and (3) the abnormal autophagic pathways present in neoplastic cells that are dependent on the lysosome [13,77].

### 3.3.10. Co-localization of Lamp2 and cathepsin D

To further examine the effect of bis(thiosemicarbazones) and their Cu complexes on the lysosome, we examined the effect of incubating SK-N-MC cells with GTSM ( $2 \mu\text{M}$ ) and  $\text{CuCl}_2$  ( $5 \mu\text{M}$ ) on the intracellular distribution of a major lysosome membrane glycoprotein [60], namely Lamp2, and the lysosomal protease, cathepsin D (Fig. 8) [58,78]. Lysosome permeabilization leads to the redistribution of cathepsin D from lysosomes into the cytosol and results in the initiation of lysosome-dependent apoptotic signaling pathways [59,79]. Cathepsin D release is an early event in the apoptotic cascade, preceding destabilization of mitochondria, and the subsequent release of cytochrome c and caspase activation [78].

In these studies, SK-N-MC cells were incubated in 3 successive steps: (1) for 10 min/37 °C with medium alone (control), or medium containing TM ( $5 \mu\text{M}$ ), or NAC ( $2 \text{ mM}$ ); or alternatively, medium alone (control), or medium containing BSO ( $100 \mu\text{M}$ ) for 16 h/37 °C; (2) medium alone or medium containing  $\text{CuCl}_2$  ( $5 \mu\text{M}$ ); and (3) GTSM ( $2 \mu\text{M}$ ) for 1 h/37 °C. Immunofluorescence microscopy was then used to examine the effects of GTSM in the presence of  $\text{CuCl}_2$  on the localization of Lamp2 (red) and cathepsin D (green; Fig. 8A). To stain nuclei, 4',6-diamidino-2-phenylindole (DAPI; blue) was used and was not markedly affected by any of the treatments (Fig. 8A). Green fluorescence intensity was also quantified using the image processing and analysis software, ImageJ v1.48 (Fig. 8B).

Untreated SK-N-MC control cells stained for Lamp2 and cathepsin D displayed a granular/vesicular pattern consistent with the labeling of lysosomes (Fig. 8A(b), (c)). Importantly, the overlay of Lamp2 (Fig. 8A(b)) and cathepsin D (Fig. 8A(c)) demonstrated a yellow punctate pattern (Fig. 8A(d)) consistent with their co-localization [59] and suggested the presence of intact lysosomes (Fig. 8A(d)). Previous studies have demonstrated that while Lamp2 is bound within the lysosomal membrane as it is an integral membrane protein [60], cathepsin D is a soluble enzyme within the lysosome [78] and can be released into the cytosol upon LMP, providing an appropriate marker for this event [59].

Incubation of SK-N-MC cells with  $\text{CuCl}_2$  alone also revealed a similar pattern of punctate vesicles, showing co-localization of Lamp2 and cathepsin D (Fig. 8A(h)). In fact, no significant ( $p > 0.05$ ) difference in green fluorescence was observed upon incubation with  $\text{CuCl}_2$  relative to the control (Fig. 8B). However, GTSM in the presence of  $\text{CuCl}_2$  led to a marked morphological alteration in Lamp2 (Fig. 8(j)) and cathepsin D (Fig. 8(k)) fluorescence relative to the respective controls (Fig. 8(b), (c)). In fact, the vesicular distribution of staining in Fig. 8(b) and (c) disappeared, and was replaced by homogenous clumps of staining (Fig. 8(j), (k)), suggesting marked damage. In fact, incubation with GTSM and  $\text{CuCl}_2$  led to a significant ( $p < 0.001$ ) loss of green cathepsin D fluorescence to  $47\% \pm 8\%$  of the control (Fig. 8B). Importantly, the overlay of Lamp2 and cathepsin D revealed a reduction in their co-localization, leading to a decrease of yellow fluorescence (Fig. 8A(l)) relative to the control (Fig. 8A(d)). This observation indicates the

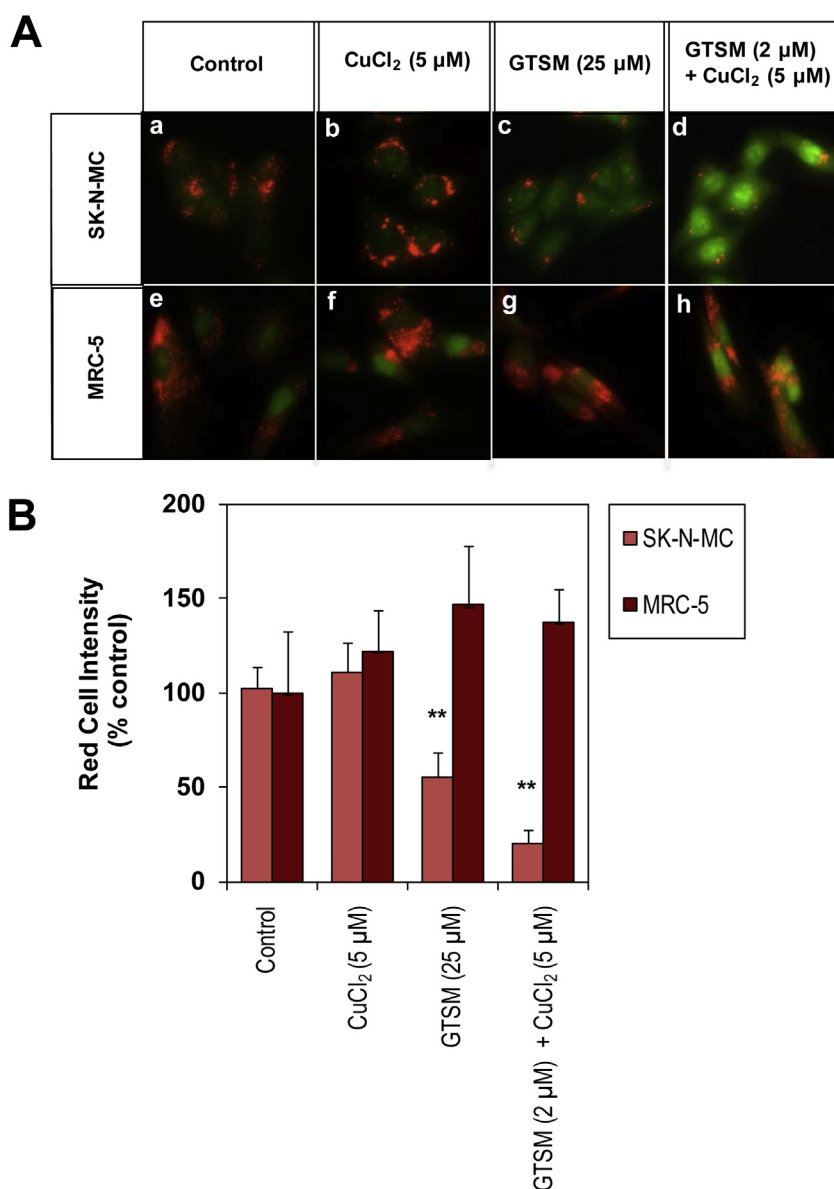


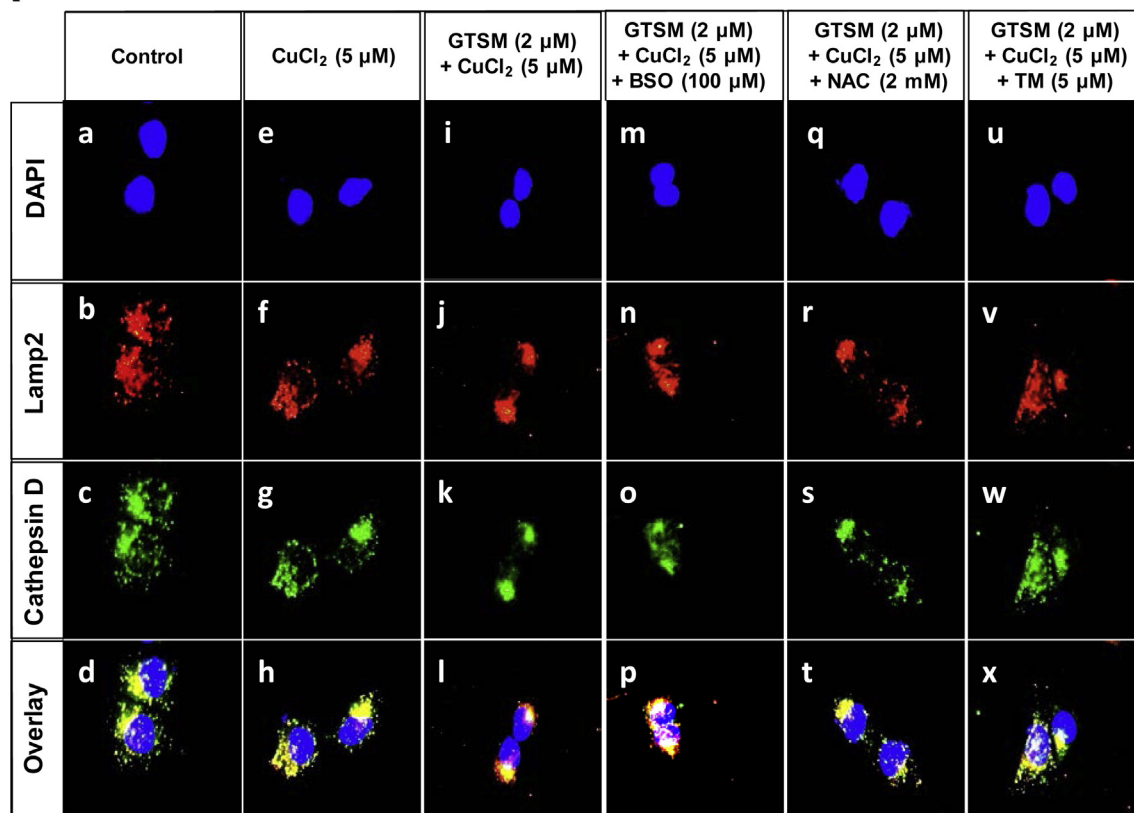
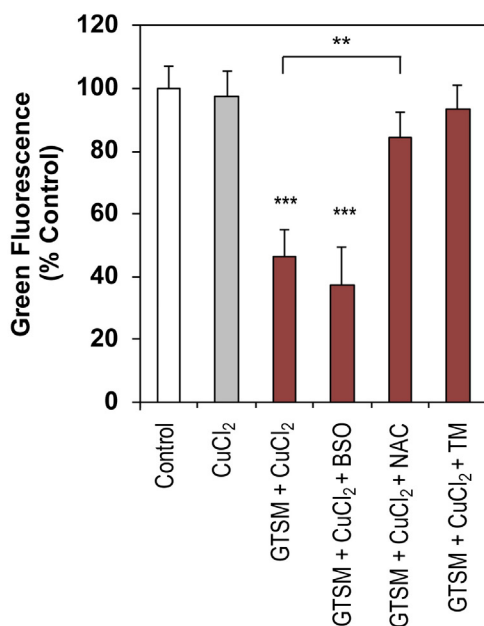
**Fig. 7.** (A) Acridine orange (AO) lysosomal stability assay comparing the sensitivity of SK-N-MC neuroepithelioma cells versus MRC-5 lung fibroblasts to lysosomal membrane permeabilization (LMP). (A) Cells were incubated with GTSM (2 or 25 μM) for 1 h/37 °C, with or without a 10 min/37 °C pre-incubation with CuCl<sub>2</sub> (5 μM); and (B) Quantification of AO (red fluorescence) with the image processing and analysis software, ImageJ v1.48. Results are typical of 3 experiments. \*\*, versus control,  $p < 0.01$ . (For interpretation of the references to color in this figure legend, the reader is referred to the web version of this article.)

redistribution of cathepsin D from the lysosome to the cytosol following LMP after GTSM and CuCl<sub>2</sub> treatment (Fig. 8A(l)). These results strongly support the previously described AO studies examining SK-N-MC cells (Figs. 6, 7) and suggests the damaging effects of GTSM and CuCl<sub>2</sub> on lysosome integrity (Fig. 9).

Pre-incubation of cells with the GSH synthesis inhibitor, BSO, prior to incubation with CuCl<sub>2</sub> and GTSM incubation, also resulted in a pronounced reduction in punctuate, vesicular staining of Lamp2 and cathepsin D (Fig. 8A(n), (o)) relative to the respective controls (Fig. 8A(b), (c)) and reduced co-localization of Lamp2 and cathepsin D when overlaid (Fig. 8A(p)) versus the control (Fig. 8A(d)). Additionally, a significant ( $p < 0.001$ ) decrease in cathepsin D green fluorescence was also observed ( $37 \pm 12\%$  of control; Fig. 8B). In contrast, pre-incubation of cells with the anti-oxidant, NAC, prior to CuCl<sub>2</sub> and GTSM incubation, helped to prevent the loss of vesicular staining of Lamp2 (Fig. 8A(r)) and cathepsin D (Fig. 8A(s)) relative to the respective controls (Fig. 8A(b), A(c)). Additionally, the overlay of Lamp2 and cathepsin D demonstrated a yellow

punctate pattern consistent with their co-localization (Fig. 8A(t)) and suggested the presence of intact lysosomes. Moreover, the levels of cathepsin D associated green fluorescence ( $84 \pm 6\%$  of control) upon pre-incubation of NAC prior to CuCl<sub>2</sub> and GTSM incubation was only slightly reduced compared to the control (Fig. 8B).

As observed with NAC, pre-incubation of cells with the Cu chelator, TM, led to similar protection from the GTSM and CuCl<sub>2</sub>-induced loss of vesicular Lamp2 (Fig. 8A(v)) and cathepsin D (Fig. 8A(w)) staining, and in fact, their co-localization was maintained (Fig. 8A(x)), relative to the respective controls (Fig. 8(A)b–d). These observations were also in good agreement with the AO studies in Fig. 6. In summary, these findings suggest that the cytotoxicity of GTSM is mediated through the formation of redox active Cu complexes that generate intracellular redox stress that can be prevented by supplementation of GSH through NAC or chelation of Cu using TM. This redox stress results in LMP resulting in the release of cathepsin D. A schematic of this mechanism is shown in Fig. 9.

**A****B**

**Fig. 8.** (A) Immunofluorescence study examining the redistribution of soluble cathepsin D protein (green) from the lysosomes (labeled with Lamp 2 (red)) to the cytosol. SK-N-MC cells were pre-incubated with medium alone or CuCl<sub>2</sub> (5 μM), and/or BSO (100 μM) for 16 h, or NAC (5 mM) or TM (5 μM) for 10 min/37 °C. Cells were then incubated with GTSM (2 μM) for 1 h/37 °C. Nuclei are labeled with DAPI (blue). (B) Quantification of cathepsin D (green fluorescence) with image processing and analysis software, ImageJ v1.48. Results are typical of 3 experiments. \*\*,  $p < 0.01$ ; \*\*\*, versus control,  $p < 0.001$ . (For interpretation of the references to color in this figure legend, the reader is referred to the web version of this article.)

#### 4. Conclusion

Bis(thiosemicarbazones) and their Cu complexes have been the focus of a variety of medical applications due to their wide range of pharmacological effects, including their anti-cancer activity [29–32]. Despite extensive study, there is an incomplete understanding of their

intracellular mechanism of action. Knowledge of their mechanisms of action is crucial to develop effective chemotherapeutics with high selectivity and minimal toxicity. In the current investigation, we examined the relationship between bis(thiosemicarbazone) structure, electrochemical behavior and anti-proliferative activity, and propose a novel mechanism of bis(thiosemicarbazone)-induced cytotoxicity.

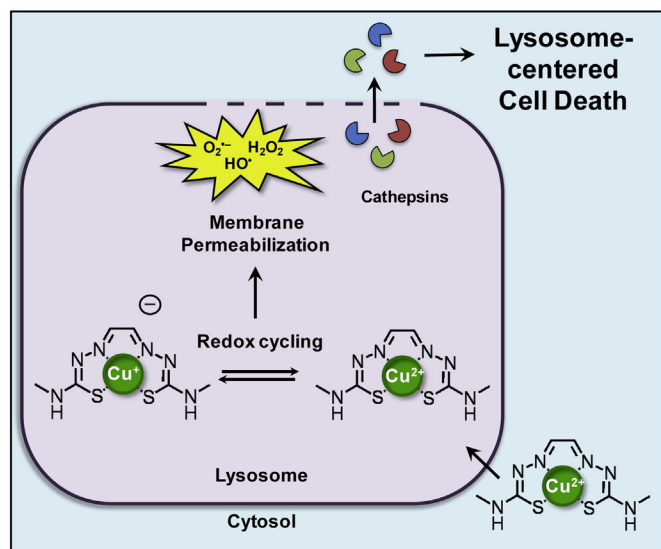


**Fig. 9.** Schematic diagram demonstrating the mechanisms of action of GTSM. GTSM is able to form redox active Cu complexes that target the lysosome to induce lysosomal membrane permeabilization, leading to the redistribution of cathepsins to the cytosol to induce apoptosis.

Synthesis of a series of bis(thiosemicarbazone) ligands and their Cu complexes revealed the importance of the alkyl substitutions at the diimine positions ( $R_1$  and  $R_2$ ) of the ligand backbone and yielded two major groups, namely, the unsubstituted/monosubstituted and disubstituted bis(thiosemicarbazones), that had distinct electrochemical and biological activity. The unsubstituted/monosubstituted ligands (GTS, GTSM, PTS and PTSM), which demonstrated less negative Cu<sup>II/I</sup> redox potentials and were more hydrophilic, exhibited potent anti-cancer activity with an appreciable *in vitro* therapeutic index and decreased <sup>64</sup>Cu release from cells. In contrast, the disubstituted ligands (ATS, ATSM, CTS, CTSM, DTS, DTSM, CyTS, CyTSM), which displayed more negative Cu<sup>II/I</sup> redox potentials and were more hydrophobic, demonstrated poor anti-proliferative activity and greater <sup>64</sup>Cu mobilization relative to their unsubstituted/monosubstituted counterparts. Significantly, the alkyl substitution pattern at the diimine positions governed their: (1) Cu<sup>II/I</sup> redox potentials; (2) ability to mediate cellular <sup>64</sup>Cu release; (3) lipophilicity; and (4) anti-proliferative activity.

Importantly, the anti-proliferative activity of these agents could be inhibited by either: (1) Cu sequestration, using the non-toxic Cu chelator, TM; or (2) supplementation of GSH levels, using NAC. Conversely, GSH depletion using BSO potentiated their anti-proliferative effects. These studies suggested the role of Cu chelation, Cu<sup>II/I</sup> redox cycling and generation of ROS in their mechanism of anti-cancer activity. This conclusion was supported by flow cytometric studies with the redox probe, DCF, which revealed significant cellular ROS generation by GTSM, which was dependent on the availability of chelatable Cu.

Morphological studies using the lysosomotropic agent, AO, indicated that the lysosome was a potentially important target of the potent anti-cancer bis(thiosemicarbazone), GTSM. Incubation of cells with GTSM in the presence of supplemental Cu led to the disappearance of AO-stained lysosomes, consistent with a relocation of AO from the lysosomes to the cytosol, following LMP. Importantly, preservation of lysosomal integrity was observed after supplementation of cellular GSH using NAC and Cu sequestration by TM. Conversely, lysosomal injury increased upon the depletion of the anti-oxidant, GSH, using the GSH synthesis inhibitor, BSO.

These results observed using AO were further supported by immunofluorescence studies examining the intracellular distribution of the well characterized lysosomal markers, Lamp2 and cathepsin D. Importantly, a decrease in co-localization of Lamp2 and cathepsin D was observed with GTSM incubation in the presence of Cu. These

investigations are consistent with a redistribution of cathepsin D from lysosomes to the cytosol following LMP. Significantly, cathepsin D release into the cytosol triggers apoptosis through their interaction with well-documented downstream effectors [27,78].

Significantly, these results suggest that bis(thiosemicarbazones), such as GTSM, behave in a similar manner to that of the thiosemicarbazone, Dp44mT, to induce their anti-cancer activity by forming redox active Cu complexes that target the lysosome to mediate LMP (Fig. 9) [26]. However, distinct differences in the structure-activity relationships of both classes of ligands are obvious [23,63,80]. Importantly, aromatic and aliphatic substitutions at the imine carbon and terminal N4 atom that result in enhanced lipophilicity played a critical role in increasing the anti-proliferative activity of thiosemicarbazones [23, 63,80]. In contrast, disubstitution of the diimine backbone of the bis(thiosemicarbazones) was detrimental to their anti-cancer activity. This suggests that the inductive effects of these substitutions on the Cu<sup>II/I</sup> redox potentials, rather than changes in their lipophilicity, played a more significant role in their anti-proliferative activity.

In summary, we propose a mechanism for bis(thiosemicarbazone)-induced cytotoxicity involving copper complexation and intracellular ROS generation, leading to LMP, the redistribution of cathepsins, and the initiation of lysosome-centered cell death pathways. Hence, lysosomal targeting of cytotoxic drugs, such as some members of the thiosemicarbazone class, is an important new therapeutic strategy that deserves further investigation.

## 5. Conflict of interest

D.R.R. is a stakeholder in the companies, Oncochel Therapeutics LLC, USA, and Oncochel Therapeutics Pty Ltd, Australia, that are developing the thiosemicarbazone, DpC, for the treatment of cancer. D.R.R. also consults for Oncochel Therapeutics LLC and Pty Ltd.

## 6. Author contributions

C.S. performed studies and wrote the manuscript; Z.A. performed studies and prepared figures; P.J. designed studies and wrote the manuscript; D.S.K. and D.R.R. designed studies and wrote the manuscript (participated as equal senior authors).

## 7. Abbreviations

3-AP	3-aminopyridine-2-carboxaldehyde thiosemicarbazone
AO	acridine orange
ATS	diacetyl bis(thiosemicarbazone)
ATSM	diacetyl bis(4-methyl-3-thiosemicarbazone)
BSO	buthionine sulfoximine
CTS	2,3-pentanedione bis(thiosemicarbazone)
CTSM	2,3-pentanedione bis(4-methyl-3-thiosemicarbazone);
CyTS	1,2-cyclohexanedione bis(thiosemicarbazone)
CyTSM	1,2-cyclohexanedione bis(4-methyl-3-thiosemicarbazone)
DCF	dichlorofluorescein
DFO	desferrioxamine
Dp44mT	di-2-pyridylketone 4,4-dimethyl-3-thiosemicarbazone
DTS	3,4-hexanedionebis(thiosemicarbazone)
DTSM	3,4-hexanedionebis(4-methyl-3-thiosemicarbazone)
GSH	glutathione
GTS	glyoxal bis(thiosemicarbazone)
GTSM	glyoxal bis(4-methyl-3-thiosemicarbazone)
H <sub>2</sub> DCF-DA	2',7'-dichlorodihydrofluorescein diacetate
H <sub>2</sub> O <sub>2</sub>	hydrogen peroxide
LMP	lysosomal membrane permeabilization
NAC	<i>N</i> -acetyl-L-cysteine;
Neo	neocuproine
PTS	pyruvaldehyde bis(thiosemicarbazone)
PTSM	pyruvaldehyde bis(4-methyl-3-thiosemicarbazone)

ROS reactive oxygen species  
TM ammonium tetrathiomolybdate

## Acknowledgments

This work was supported by a Project Grant from the National Health and Medical Research Council (NHMRC) Australia to D.R.R. [1021607] and D.S.K. [1048972]; a NHMRC Senior Principal Research Fellowship to D.R.R. [1062607]; a NHMRC RD Wright Fellowship to D.S.K. [1083057]; and a Helen and Robert Ellis Fellowship to D.S.K. from the Sydney Medical School Foundation of The University of Sydney. P.J.J. (10/CDF/2-15) thanks the Cancer Institute NSW for Fellowship support. C.S. is the grateful recipient of an Australian Postgraduate Award from the University of Sydney.

## References

- [1] Z.L. Harris, J.D. Gitlin, *Am. J. Clin. Nutr.* 63 (1996) S836–S841.
- [2] V.L. Goodman, G.J. Brewer, S.D. Merajver, *Endocr. Relat. Cancer* 11 (2004) 255–263.
- [3] H.W. Kuo, S.F. Chen, C.C. Wu, D.R. Chen, J.H. Lee, *Biol. Trace Elem. Res.* 89 (2002) 1–11.
- [4] S. Apelt, J. Coppey, A. Fromentin, E. Guille, M.F. Poupon, A. Roussel, *Anticancer Res.* 6 (1986) 159–164.
- [5] S. Taysi, F. Akcay, C. Uslu, Y. Dogru, I. Gulcin, *Biol. Trace Elem. Res.* 91 (2003) 11–18.
- [6] A. Chan, F. Wong, M. Arumanayagam, *Ann. Clin. Biochem.* 30 (1993) 545–549.
- [7] M.C. Linder, J.R. Moor, K. Wright, *J. Natl. Cancer Inst.* 67 (1981) 263–275.
- [8] F.K. Habib, T.C. Dembinski, S.R. Stitch, *Clin. Chim. Acta* 104 (1980) 329–335.
- [9] S.K. Gupta, V.K. Shukla, M.P. Vaidya, S.K. Roy, S. Gupta, *J. Surg. Oncol.* 46 (1991) 178–181.
- [10] U. Carpentieri, J. Myers, L. Thorpe, C.W. Daeschner III, M.E. Haggard, *Cancer Res.* 46 (1986) 981–984.
- [11] A. Gupte, R.J. Mumper, *Cancer Treat. Rev.* 35 (2009) 32–46.
- [12] T. Wang, Z.J. Guo, *Curr. Med. Chem.* 13 (2006) 525–537.
- [13] F. Tisato, C. Marzano, M. Porchia, M. Pellei, C. Santini, *Med. Res. Rev.* 30 (2010) 708–749.
- [14] C.R. Kowol, P. Heffeter, W. Miklos, L. Gille, R. Trondl, L. Cappellacci, W. Berger, B.K. Keppler, *J. Biol. Inorg. Chem.* 17 (2012) 409–423.
- [15] D. Trachootham, J. Alexandre, P. Huang, *Nat. Rev. Drug Discov.* 8 (2009) 579–591.
- [16] Y. Yu, D.S. Kalinowski, Z. Kovacevic, A.R. Siafakas, P.J. Jansson, C. Stefani, D.B. Lovejoy, P.C. Sharpe, P.V. Bernhardt, D.R. Richardson, *J. Med. Chem.* 52 (2009) 5271–5294.
- [17] R.A. Finch, M.C. Liu, S.P. Grill, W.C. Rose, R. Loomis, K.M. Vasquez, Y.C. Cheng, A.C. Sartorelli, *Biochem. Pharmacol.* 59 (2000) 983–991.
- [18] J.S. Casas, M.S. Garcia-Tasende, J. Sordo, *Coord. Chem. Rev.* 209 (2000) 197–261.
- [19] M. Whitnall, J. Howard, P. Ponka, D.R. Richardson, *Proc. Natl. Acad. Sci. U. S. A.* 103 (2006) 14901–14906.
- [20] J.L.J. Dearling, J.S. Lewis, G.E.D. Muller, M.J. Welch, P.J. Blower, *J. Biol. Inorg. Chem.* 7 (2002) 249–259.
- [21] S.N. Pandeya, D. Sriram, G. Nath, E. DeClercq, *Eur. J. Pharm. Sci.* 9 (1999) 25–31.
- [22] J. Yuan, D.B. Lovejoy, D.R. Richardson, *Blood* 104 (2004) 1450–1458.
- [23] D.R. Richardson, P.C. Sharpe, D.B. Lovejoy, D. Senaratne, D.S. Kalinowski, M. Islam, P.V. Bernhardt, *J. Med. Chem.* 49 (2006) 6510–6521.
- [24] P.J. Jansson, C.L. Hawkins, D.B. Lovejoy, D.R. Richardson, *J. Inorg. Biochem.* 104 (2010) 1224–1228.
- [25] P.J. Jansson, P.C. Sharpe, P.V. Bernhardt, D.R. Richardson, *J. Med. Chem.* 53 (2010) 5759–5769.
- [26] D.B. Lovejoy, P.J. Jansson, U.T. Brunk, J. Wong, P. Ponka, D.R. Richardson, *Cancer Res.* 71 (2011) 5871–5880.
- [27] N. Fehrenbacher, L. Bastholm, T. Kirkegaard-Sorensen, B. Rafn, T. Bottzauw, C. Nielsen, E. Weber, S. Shirasawa, T. Kallunki, M. Jaattela, *Cancer Res.* 68 (2008) 6623–6633.
- [28] T. Kallunki, O.D. Olsen, M. Jaattela, *Oncogene* 32 (2013) 1995–2004.
- [29] F.A. French, B.L. Freedlander, *Cancer Res.* 18 (1958) 172–175.
- [30] F.A. French, B.L. Freedlander, *Cancer Res.* 18 (1958) 1290–1300.
- [31] V.C. Barry, M.L. Conalty, J.F. Osullivan, *Cancer Res.* 26 (1966) 2165–2170.
- [32] B.A. Booth, A.C. Sartorelli, *Nature* 210 (1966) 104–109.
- [33] H.G. Petering, G.J. VanGiessen, J.A. Crim, H.H. Buskirk, *J. Med. Chem.* 9 (1966) 420–425.
- [34] D. Kessel, R.S. McElhinney, *Mol. Pharmacol.* 11 (1975) 298–309.
- [35] J.A. Crim, H.G. Petering, *Cancer Res.* 27 (1967) 1278–1285.
- [36] J.L.J. Dearling, J.S. Lewis, D.W. McCarthy, M.J. Welch, P.J. Blower, *Chem. Commun.* (1998) 2531–2532.
- [37] Y. Fujibayashi, H. Taniuchi, Y. Yonekura, H. Ohtani, J. Konishi, A. Yokoyama, *J. Nucl. Med.* 38 (1997) 1155–1160.
- [38] R.I. Maurer, P.J. Blower, J.R. Dilworth, C.A. Reynolds, Y. Zheng, G.E. Mullen, *J. Med. Chem.* 45 (2002) 1420–1431.
- [39] T.C. Castle, R.I. Maurer, F.E. Sowrey, M.J. Went, C.A. Reynolds, E.J.L. McInnes, P.J. Blower, *J. Am. Chem. Soc.* 125 (2003) 10040–10049.
- [40] P.J. Blower, T.C. Castle, A.R. Cowley, J.R. Dilworth, P.S. Donnelly, E. Labisbal, F.E. Sowrey, S.J. Teat, M.J. Went, *Dalton Trans.* (2003) 4416–4425.
- [41] P.J. Blower, J.R. Dilworth, R.I. Maurer, G.D. Mullen, C.A. Reynolds, Y. Zheng, *J. Inorg. Biochem.* 85 (2001) 15–22.
- [42] F. Dehdashti, P.W. Grigsby, J.S. Lewis, R. Laforest, B.A. Siegel, M.J. Welch, *J. Nucl. Med.* 49 (2008) 201–205.
- [43] D.W. Dietz, F. Dehdashti, P.W. Grigsby, R.S. Malyapa, R.J. Myerson, J. Picus, J. Ritter, J.S. Lewis, M.J. Welch, B.A. Siegel, *Dis. Colon Rectum* 51 (2008) 1641–1648.
- [44] S.I. Pascu, P.A. Waghorn, T.D. Conry, B. Lin, H.M. Betts, J.R. Dilworth, R.B. Sim, G.C. Churchill, F.I. Aigbirhio, J.E. Warren, *Dalton Trans.* (2008) 2107–2110.
- [45] S. Lim, K.A. Price, S.F. Chong, B.M. Paterson, A. Caragounis, K.J. Barnham, P.J. Crouch, J.M. Peach, J.R. Dilworth, A.R. White, P.S. Donnelly, *J. Biol. Inorg. Chem.* 15 (2010) 225–235.
- [46] S.I. Pascu, P.A. Waghorn, B.W. Kennedy, R.L. Arrowsmith, S.R. Bayly, J.R. Dilworth, M. Christlieb, R.M. Tyrrell, J. Zhong, R.M. Kowalczyk, D. Collison, P.K. Aley, G.C. Churchill, F.I. Aigbirhio, *Chem. Asian. J.* 5 (2010) 506–519.
- [47] D. Dayal, D. Palanimuthu, S.V. Shinde, K. Somasundaram, A.G. Samuelson, *J. Biol. Inorg. Chem.* 16 (2011) 621–632.
- [48] K.A. Price, P.J. Crouch, S. Lim, B.M. Paterson, J.R. Liddell, P.S. Donnelly, A.R. White, *Metallomics* 3 (2011) 1280–1290.
- [49] P.V. Bernhardt, L.M. Caldwell, T.B. Chaston, P. Chin, D.R. Richardson, *J. Biol. Inorg. Chem.* 8 (2003) 866–880.
- [50] M.C. Liu, T.S. Lin, A.C. Sartorelli, *J. Med. Chem.* 35 (1992) 3672–3677.
- [51] A.K. Ghose, G.M. Crippen, *J. Chem. Inf. Comput. Sci.* 27 (1987) 21–35.
- [52] D.R. Richardson, E.H. Tran, P. Ponka, *Blood* 86 (1995) 4295–4306.
- [53] D.R. Richardson, K. Milnes, *Blood* 89 (1997) 3025–3038.
- [54] O.I. Aromoa, B. Halliwell, B.M. Hoey, J. Butler, *Free Radic. Biol. Med.* 6 (1989) 593–597.
- [55] H.U. Simon, A. Haj-Yehia, F. Levi-Schaffer, *Apoptosis* 5 (2000) 415–418.
- [56] J. Liu, A. Hajibeigi, G. Ren, M. Lin, W. Siyambalapatiyage, Z. Lium, E. Simpson, R.W. Parkey, X. Sun, O.K. Oz, *J. Nuclear. Med.* 50 (2009) 1332–1339.
- [57] O. Myhre, J.M. Andersen, H. Aarnes, F. Fonnum, *Biochem. Pharmacol.* 65 (2003) 1575–1582.
- [58] H.J. Yu, Y.F. Zhou, S.E. Lind, W.Q. Ding, *Biochem. J.* 417 (2009) 133–139.
- [59] P.J. Jansson, T. Yamagishi, A. Arvind, N. Seebacher, E. Gutierrez, A. Stacy, S. Maleki, D. Sharp, S. Sahni, D.R. Richardson, *J. Biol. Chem.* 290 (2015) 9588–9603.
- [60] E.L. Eskelinen, *Mol. Asp. Med.* 27 (2006) 495–502.
- [61] T. Yamagishi, S. Sahni, D.M. Sharp, A. Arvind, P.J. Jansson, D.R. Richardson, *J. Biol. Chem.* 288 (2013) 31761–31771.
- [62] Q. Pan, C.G. Kleer, K.L. van Golen, J. Irani, K.M. Bottema, C. Bias, M. De Carvalho, E.A. Mesri, D.M. Robins, R.D. Dick, G.J. Brewer, S.D. Merajver, *Cancer Res.* 62 (2002) 4854–4859.
- [63] D.S. Kalinowski, Y. Yu, P.C. Sharpe, M. Islam, Y.T. Liao, D.B. Lovejoy, N. Kumar, P.V. Bernhardt, D.R. Richardson, *J. Med. Chem.* 50 (2007) 3716–3729.
- [64] D.S. Kalinowski, D.R. Richardson, *Pharmacol. Rev.* 57 (2005) 547–583.
- [65] J.E. Karp, F.J. Giles, I. Gojo, L. Morris, J. Greer, B. Johnson, M. Thein, M. Sznol, *J. Low. Leuk. Res.* 32 (2008) 71–77.
- [66] B. Ma, B.C. Goh, E.H. Tan, K.C. Lam, R. Soo, S.S. Leong, L.Z. Wang, F. Mo, A.T. Chan, B. Zee, T. Mok, *Investig. New Drugs* 26 (2008) 169–173.
- [67] M.J. Mackenzie, D. Saltman, H. Hirte, J. Low, C. Johnson, G. Pond, M.J. Moore, *Investig. New Drugs* 25 (2007) 553–558.
- [68] D. Palanimuthu, S.V. Shinde, K. Somasundaram, A.G. Samuelson, *J. Med. Chem.* 56 (2013) 722–734.
- [69] P.S. Donnelly, A. Caragounis, T. Du, K.M. Laughton, I. Volitakis, R.A. Cherny, R.A. Sharples, A.F. Hill, Q.X. Li, C.L. Masters, K.J. Barnham, A.R. White, *J. Biol. Chem.* 283 (2008) 4568–4577.
- [70] H. Tapiero, D.M. Townsend, K.D. Tew, *Biomed. Pharmacother.* 57 (2003) 386–398.
- [71] P. Ubezio, F. Civoli, *Free Radic. Biol. Med.* 16 (1994) 509–516.
- [72] M. Karlsson, T. Kurz, U.T. Brunk, S.E. Nilsson, C.I. Frennesson, *Biochem. J.* 428 (2010) 183–190.
- [73] E. Gutierrez, D.R. Richardson, P.J. Jansson, *J. Biol. Chem.* 289 (2014) 33568–33589.
- [74] H. Erdal, M. Berndtsson, J. Castro, U. Brunk, M.C. Shoshan, S. Linder, *Proc. Natl. Acad. Sci. U. S. A.* 102 (2005) 192–197.
- [75] C.B. Thompson, *Science* 267 (1995) 1456–1462.
- [76] S. Aits, M. Jaattela, *J. Cell Sci.* 126 (2013) 1905–1912.
- [77] N. Chen, V. Karantza-Wadsworth, *Biochim. Biophys. Acta* 1793 (2009) 1516–1523.
- [78] P. Benes, V. Vetvicka, M. Fusek, *Crit. Rev. Oncol. Hematol.* 68 (2008) 12–28.
- [79] P. Boya, G. Kroemer, *Oncogene* 27 (2008) 6434–6451.
- [80] D.B. Lovejoy, D.M. Sharp, N. Seebacher, P. Obeidy, T. Prichard, C. Stefani, M.T. Basha, P.C. Sharpe, P.J. Jansson, D.S. Kalinowski, P.V. Bernhardt, D.R. Richardson, *J. Med. Chem.* 55 (2012) 7230–7244.